Tectonics®

RESEARCH ARTICLE
10.1029/2021TC007060

Key Points:

- End-on latest Triassic to Early Jurassic arc-continent collision in the northern Cordillera
- Crustal thickening and syn-collisional magmatism north of Stikine arch linked by transform faults to retreating Hazelton slab to the south
- Southward slab retreat and transform faults result in entrapment of the Cache Creek terrane

Correspondence to:
M. Colpron,
maurice.colpron@yukon.ca

Citation:
Colpron, M., Sack, P. J., Crowley, J. L., Beranek, L. P., & Allan, M. M. (2022). Late Triassic to Jurassic magmatic and tectonic evolution of the Intermontane terranes in Yukon, northern Canadian Cordillera: Transition from arc to syn-collisional magmatism and post-collisional lithospheric delamination. *Tectonics*, *41*, e2021TC007060. https://doi.org/10.1029/2021TC007060

Received 9 OCT 2021
Accepted 31 JAN 2022

Author Contributions:
Conceptualization: Maurice Colpron, Patrick J. Sack
Formal analysis: Maurice Colpron, Patrick J. Sack, James L. Crowley, Luke P. Beranek, Murray M. Allan
Funding acquisition: Maurice Colpron, Patrick J. Sack
Investigation: Maurice Colpron, Patrick J. Sack, James L. Crowley, Murray M. Allan
Methodology: Maurice Colpron, Patrick J. Sack, James L. Crowley, Luke P. Beranek, Murray M. Allan
Project Administration: Maurice Colpron, Patrick J. Sack
Validation: Patrick J. Sack
Writing – original draft: Maurice Colpron
Writing – review & editing: Patrick J. Sack, James L. Crowley, Luke P. Beranek, Murray M. Allan

Late Triassic to Jurassic Magmatic and Tectonic Evolution of the Intermontane Terranes in Yukon, Northern Canadian Cordillera: Transition From Arc to Syn-Collisional Magmatism and Post-Collisional Lithospheric Delamination

Maurice Colpron[1], Patrick J. Sack[1], James L. Crowley[2], Luke P. Beranek[3], and Murray M. Allan[4,5]

[1]Yukon Geological Survey, Whitehorse, YT, Canada, [2]Department of Geosciences, Boise State University, Boise, ID, USA, [3]Department of Earth Sciences, Memorial University of Newfoundland, St. John's, NL, Canada, [4]Mineral Deposit Research Unit, Department of Earth, Ocean and Atmospheric Sciences, The University of British Columbia, Vancouver, BC, Canada, [5]Now at Teck Resources Limited, Vancouver, BC, Canada

Abstract End-on arc collision and onset of the northern Cordilleran orogen is recorded in Late Triassic to Jurassic plutons in the Intermontane terranes of Yukon, and in development of the synorogenic Whitehorse trough (WT). A synthesis of the extensive data set for these plutons supports interpretation of the magmatic and tectonic evolution of the northern Intermontane terranes. Late Triassic juvenile plutons that locally intrude the Yukon-Tanana terrane represent the northern extension of arc magmatism within Stikinia. Early Jurassic plutons that intrude Stikinia and Yukon-Tanana terranes were emplaced during crustal thickening (200–195 Ma) and subsequent exhumation (190–178 Ma). The syn-collisional magmatism migrated to the south and shows increasing crustal contributions with time. This style of magmatism in Yukon contrasts with coeval, juvenile arc magmatism in British Columbia (Hazelton Group), that records southward arc migration in the Early Jurassic. Exhumation and subsidence of the WT in the north were probably linked to the retreating Hazelton arc by a sinistral transform. East of WT, Early Jurassic plutons intruded into Yukon-Tanana record continued arc magmatism in Quesnellia. Middle Jurassic plutons were intruded after final enclosure of the Cache Creek terrane and imbrication of the Intermontane terranes. The post-collisional plutons have juvenile isotopic compositions that, together with stratigraphic evidence of surface uplift, are interpreted to record asthenospheric upwelling and lithospheric delamination. A revised tectonic model proposes that entrapment of the Cache Creek terrane was the result of Hazelton slab rollback and development of a sinistral transform fault system linked to the collision zone to the north.

1. Introduction

Crustal growth at convergent margins is generally thought to occur through accretion of juvenile arc crust and/or addition of magmatic material to the edge of a craton (e.g., Rudnick, 1995). Arc-continent collision zones are thus major sites for crustal growth through time (e.g., Brown et al., 2011). Arc accretion generally leads to development of an accretionary orogen, associated magmatism and basin(s) (e.g., Cawood et al., 2009; Draut & Clift, 2012). The evolution of arc-continent collision zones is generally complex and shows a wide-range of variations depending on configuration of continental and arc crusts, and angle and rates of convergence (Brown et al., 2011). There is no simple model that explains the variations observed in modern and ancient arc-continent collisions.

In western North America, the development of the northern Cordilleran accretionary orogen began with collision of early Mesozoic peri-Laurentian arcs with the continental margin in latest Triassic to Early Jurassic (Colpron et al., 2015; George et al., 2021; Monger & Nokleberg, 1996; Monger & Price, 2002; Nelson et al., 2013). Initial accretion involved the Intermontane terranes (Figure 1), which occupy the core of the orogen in Canada and include a series of magmatic arcs (Stikinia, Quesnellia, and Yukon-Tanana), marginal ocean basins (Slide Mountain), and accretionary complexes (Cache Creek) that evolved at the western edge of the Laurentian plate (ancestral North America) between mid-Paleozoic and early Mesozoic (Colpron et al., 2007; Monger et al., 1982; Nelson et al., 2013). The Late Triassic magmatic arcs of Quesnellia and Stikinia are generally interpreted to have formed part of a contiguous arc system that was duplicated during Early to Middle Jurassic accretion, either as a consequence of strike-slip faulting (Wernicke & Klepacki, 1988) or oroclinal bending (Mihalynuk et al., 1994, 2004;

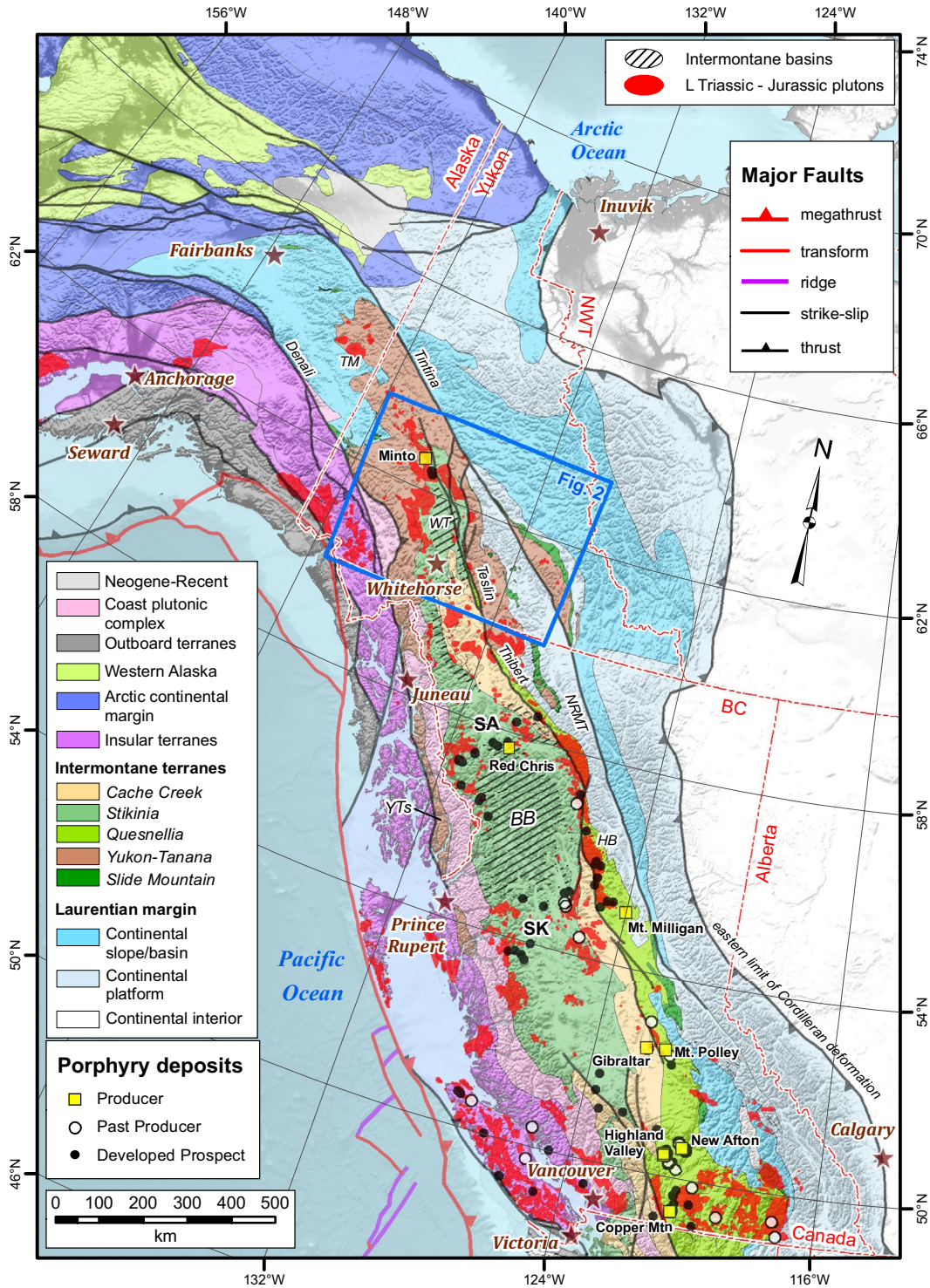

Figure 1. Late Triassic to Jurassic plutons and significant Cu ± Au(±Mo) porphyry deposits of the northern Cordillera. Selected producing mines are labeled. Simplified terrane map modified after Colpron and Nelson (2011). Plutons are from Cui et al. (2017) for British Columbia, Yukon Geological Survey (2020a) for Yukon, and Wilson et al. (2015) for Alaska. Selected porphyry deposits are from BC MINFILE (British Columbia Geological Survey, 2019) and Yukon MINFILE (Yukon Geological Survey, 2020b) databases. *Abbreviations*. BB, Bowser basin; HB, Hogem batholith; Mt., Mount; Mtn., Mountain; NRMT, Northern Rocky Mountain Trench; SA, Stikine arch; SK, Skeena arch; TM, Taylor Mountain batholith; YTs, Yukon-Tanana south; WT, Whitehorse trough.

Nelson & Mihalynuk, 1993). This resulted in entrapment of the Cache Creek terrane—the accretionary complex and related arc and oceanic rocks that developed in the forearc of Stikinia and Quesnellia (Monger, 1977; Monger et al., 1982; Travers, 1978). There is increasing evidence that arc-continent collision and crustal thickening first occurred in the latest Triassic-earliest Jurassic in the northern Intermontane terranes north of the Stikine arch (Figure 1) and was followed by Early Jurassic exhumation of Stikinia and the Yukon-Tanana terranes in Yukon. Evidence of latest Triassic to Early Jurassic tectonism include: (a) folding of Late Triassic strata and development of regional Early Jurassic unconformities (Brown et al., 1996; George et al., 2021; Greig, 2014; Greig & Gehrels, 1995); (b) ca. 205–195 Ma amphibolite-facies regional metamorphism in rocks of the Yukon-Tanana terrane (Clark, 2017; Gaidies et al., 2021); and (c) widespread Early Jurassic mica cooling ages in metamorphic rocks of the Yukon-Tanana terrane (Colpron et al., 2015). The Early to Middle Jurassic Whitehorse trough (WT) was developed as a synorogenic piggyback basin atop this nascent orogen, and its sediments were sourced from locally exhumed rocks of Stikinia and Yukon-Tanana terranes and their contained intrusions (Colpron et al., 2015; van Drecht, 2019). Initial encroachment of the accreted terranes onto the western North American margin is constrained by Early Jurassic syn-tectonic, Alaskan-type intrusions in Quesnellia (Murphy et al., 1995; Nixon et al., 1997, 2020), and initial subsidence of the Alberta foreland basin that contains strata with syn-depositional detrital zircons (Sinemurian-Toarcian; Asgar-Deen, 2003; McCartney, 2012; Pană et al., 2018). The demise of the early Mesozoic peri-Laurentian arcs and initial growth of the Cordilleran orogen in the latest Triassic to Early Jurassic was apparently related to the westward drift of the North American continent during breakup of the supercontinent Pangea and subsequent opening of the central Atlantic Ocean (Coney, 1972; Dickinson, 2004; Monger & Gibson, 2019).

Between Late Triassic and Late Jurassic, the evolution of this arc-continent collision was accompanied by intrusion of granitoid plutons (Armstrong, 1988; Nelson et al., 2013; Wheeler & McFeely, 1991; Woodsworth et al., 1991). The Late Triassic to Early Jurassic plutons broadly form two parallel belts that extend the length of Quesnellia and Stikinia in British Columbia and converge in the Yukon-Tanana terrane of central Yukon and eastern Alaska (Figures 1 and 2). They have generally been considered arc plutons related to coeval juvenile volcanism in Stikinia and Quesnellia (e.g., Dostal et al., 2001; Logan & Mihalynuk, 2014), but plutons in Yukon have received limited attention to date. In this contribution, we present a synthesis and interpretation of the extensive data set compiled by Sack et al. (2020) in their *Atlas of Late Triassic to Jurassic plutons in the Intermontane terranes of Yukon*. The Atlas presents a systematic description of most Late Triassic to Jurassic plutons exposed between latitudes 60°N and 63°15′N in southern Yukon (Figure 2). This data set is anchored on 35 high-precision U-Pb zircon dates and associated geochemical and isotopic data that allow for a detailed analysis of magmatism within the arc-continent collision zone in Yukon. The integrated data set provides means to refine terrane boundaries in Yukon, more specifically between Stikinia and Quesnellia, and to test current tectonic models. Our analysis shows that Late Triassic to Jurassic plutons in Yukon record a transition from arc, to syn- and post-collision magmatism that is distinct from continued, juvenile arc magmatism in British Columbia (George et al., 2021). Together with recent studies of Late Triassic to Jurassic sedimentary and volcanic strata in British Columbia and Yukon (Colpron et al., 2015; George et al., 2021; Nelson et al., 2022; van Drecht, 2019) our synthesis provides the basis for a revised tectonic model for the early Mesozoic development of the northern Cordilleran accretionary orogen. Our model provides another example for the evolution of an ancient arc-continent collision and subsequent development of an accretionary orogen.

2. Accretionary History of the Intermontane Terranes

The Intermontane terranes are primarily composed of a series of superposed magmatic arc successions ranging from Late Devonian to Early Jurassic. The oldest of the Intermontane terranes in Yukon is the Yukon-Tanana terrane, which includes three arc successions of Late Devonian to middle Permian age (Finlayson, Klinkit, and Klondike assemblages) that were developed on top of a pre-Devonian metasedimentary succession (Snowcap assemblage; Colpron, et al., 2007; Colpron, Nelson, & Murphy, 2006; Colpron, Mortensen, et al., 2006; Mortensen, 1992; Mortensen & Jilson, 1985). The Snowcap assemblage is interpreted as a rifted fragment of the western Laurentian continental margin (Piercey & Colpron, 2009). Arc successions in the Yukon-Tanana terrane comprise two main pulses of felsic magmatism at 365–330 and 264–254 Ma, and an intervening mafic volcanic succession (Colpron, Nelson, & Murphy, 2006; Colpron, Mortensen, et al., 2006; Nelson et al., 2006). The Mississippian to early Permian mafic volcanic and carbonate rocks of the Klinkit assemblage are correlated

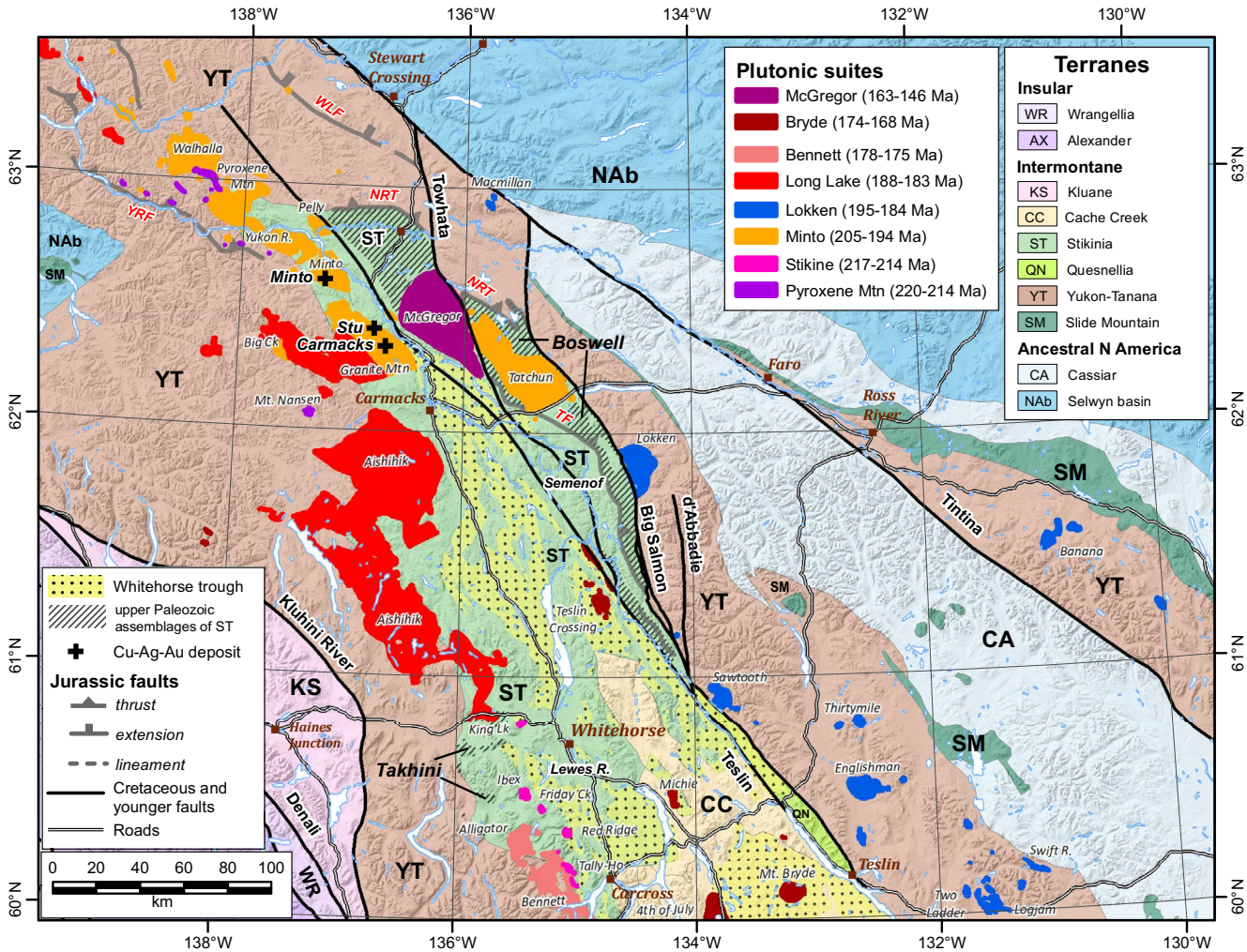

Figure 2. Distribution of Late Triassic to Jurassic plutons in the Intermontane terranes of southern Yukon. The names of plutons described in the Atlas of Sack et al. (2020) are indicated. General locations of Paleozoic (Takhini, Boswell) and Triassic (Lewes River, Semenof) assemblanges of Stikinia are also indicated. Terrane map is modified after Colpron and Nelson (2011). Plutons and distribution of Whitehorse trough strata are from Yukon Geological Survey (2020a). Jurassic faults (red labels). *Abbreviations*. NRT, Needlerock thrust; TF, Tadru fault; WLF, Willow Lake fault; YRF, Yukon River fault. *Abbreviations*. Lk, lake; Mtn, mountain; R., river.

with Paleozoic arc sequences of Quesnellia in British Columbia (Lay Range and Harper Ranch assemblages; Beatty et al., 2006; Ferri, 1997), leading to the interpretation that Yukon-Tanana is locally the basement to Mesozoic Quesnellia (Colpron et al., 2007; Nelson & Friedman, 2004; Nixon et al., 2020; Roots et al., 2006; Simard et al., 2003).

Arc development in the Yukon-Tanana terrane was coeval with opening of the Slide Mountain back-arc ocean between Late Devonian and early Permian (Colpron et al., 2007; Colpron et al., 2009; Creaser et al., 1999; Mortensen, 1992; Nelson et al., 2006). Closure of the Slide Mountain ocean is recorded in ca. 270–255 Ma eclogite at the eastern edge of Yukon-Tanana terrane (e.g., Creaser, Heaman, & Erdmer, 1997; Erdmer et al., 1998; Gilotti et al., 2017; Petrie et al., 2016) and ca. 264–254 Ma magmatism of the Klondike assemblage (Mortensen, 1990, 1992). By Middle to Late Triassic, siliciclastic rocks, derived in part from the Yukon-Tanana terrane and the Laurentian craton, overlap Yukon-Tanana, Quesnellia, Slide Mountain, and the western North American margin and indicate that the Slide Mountain Ocean had closed by that time (e.g., Beranek & Mortensen, 2011; Unterschutz et al., 2002).

The oldest rocks in Stikinia are also Paleozoic arc successions; these are distinctly more primitive in character and of uncertain relationship with coeval arc magmatism in the Yukon-Tanana terrane. In northwest British Columbia, the Stikine assemblage comprises Devonian to Permian volcanic and volcaniclastic rocks of primitive

arc affinity, associated Late Devonian to Early Mississippian calc-alkaline plutons, and Carboniferous to lower Permian (Cisuralian) limestone (Gunning et al., 2006; Logan et al., 2000; Monger, 1977). Correlative rocks in southern Yukon include metamorphosed volcanic, volcaniclastic, and minor carbonate rocks of the Pennsylvanian-Permian Takhini assemblage (Hart, 1997). Takhini metabasites have the geochemical characteristics of primitive island arc tholeiites (Bordet et al., 2019). In central Yukon, east of Carmacks (Figure 2), the Boswell assemblage includes: (a) a lower unit of Upper Devonian to Lower Mississippian basalt (normal and enriched mid-ocean ridge basalt [MORB]) and limestone and (b) an upper unit of Upper Mississippian to lower Permian arc volcanic, volcaniclastic, and sedimentary rocks (including Pennsylvanian-Permian fossiliferous limestone and Pennsylvanian tonalite and rhyolite; Colpron, 2011; Simard, 2003; Simard & Devine, 2003). These rocks were previously assigned to Quesnellia (e.g., Colpron, 2011; Gordey & Makepeace, 2001) but are considered part of Stikinia in this article for reasons discussed below.

Volcanic components of the Upper Triassic successions of Quesnellia and Stikinia are predominantly augite-phyric basalt and andesite with primitive arc geochemical and isotopic signatures (Bordet et al., 2019; Dostal et al., 1999). The similar Upper Triassic stratigraphy and petrogenesis in these two terranes suggest that they formed parts of a common Late Triassic arc system that is now duplicated as the result of Early Jurassic oroclinal bending (Mihalynuk et al., 1994) and/or strike-slip faulting (Wernicke & Klepacki, 1988). In British Columbia, Upper Triassic to Lower Jurassic rocks of Stikinia and Quesnellia occur on either side of the Cache Creek terrane, the accretionary complex that developed adjacent to the arc terranes (Figure 1; Monger, 1977; Travers, 1978). In southern Yukon, the Cache Creek terrane terminates near 61°N latitude (Figure 2; Bickerton et al., 2020) and similar Upper Triassic strata of Stikinia occur continuously around its northern end.

The Cache Creek terrane includes fragments of primitive arc crust, seamounts with Pennsylvanian-Permian limestone caps (locally with early Permian fusilinids of Tethyan affinity; Monger & Ross, 1971; Ross & Ross, 1983), extensive late Permian (Lopingian) to Middle Triassic supra-subduction zone ophiolites, pelagic sedimentary rocks, and synorogenic clastic rocks with protolith ages ranging from Mississippian to Early Jurassic (Cordey, 2020; Cordey et al., 1991; McGoldrick et al., 2017; Mihalynuk et al., 2004; Monger, 1977).

The Lower to Middle Jurassic clastic sedimentary rocks of the WT (Laberge Group) overlap Stikinia and Cache Creek terranes in Yukon and northern British Columbia (Colpron et al., 2015; English et al., 2005; Hart, 1997; Mihalynuk et al., 1999; Wheeler, 1961). Correlative strata are also locally unconformable on metamorphic rocks of the Yukon-Tanana terrane (Colpron et al., 2015). In British Columbia, coeval volcanic-sedimentary strata in Stikinia south of the Stikine arch (Figure 1) are assigned to the uppermost Triassic to Middle Jurassic, arc-related Hazelton Group (Gagnon et al., 2012; Nelson et al., 2018; Tipper & Richards, 1976).

Late Triassic to Early Jurassic plutons intrude the length of Stikinia and Quesnellia, and the Yukon-Tanana terrane in Yukon and eastern Alaska (Figures 1 and 2; Colpron, Israel, & Friend, 2016; Cui et al., 2017; Wilson et al., 2015; Woodsworth et al., 1991). These plutons are closely associated with coeval arc volcanic rocks and porphyry Cu-Au(-Mo) deposits in British Columbia (Figure 1; Logan & Mihalynuk, 2014; Mortensen et al., 1995; Nelson et al., 2013). In Yukon, Late Triassic plutons are inferred to be subvolcanic feeders to basaltic andesite of the Lewes River Group, but the younger, Early Jurassic plutons lack direct association with coeval volcanism, and Lower Jurassic volcanic rocks are limited to local tuff horizons within the Laberge Group (Colpron & Friedman, 2008; Hart, 1997; Johannson et al., 1997; Tempelman-Kluit, 1984, 2009). Detrital zircon ages and clast compositions in strata of the Laberge Group indicate that the Late Triassic to Early Jurassic plutons exposed on the flanks of WT were major, local sediment sources that were exhumed during marine deposition (Colpron et al., 2015; Dickie & Hein, 1995; Hart et al., 1995; Shirmohammad et al., 2011; van Drecht, 2019). The Laberge Group is unconformably overlain by fluvial and lacustrine strata of the Upper Jurassic to Lower Cretaceous Tantalus Formation, which are interpreted to have been deposited in confined intermontane valleys (Long, 2015; Tempelman-Kluit, 1984, 2009).

Strata of the Intermontane terranes were folded and imbricated by east-dipping, west-verging thrust faults prior to intrusion of Middle to Late Jurassic plutons (Gabrielse, 1998; Mihalynuk et al., 2004; Tipper, 1978). In Yukon, these plutons define a central belt that stitches Stikinia, Cache Creek, and WT west of the Teslin fault (Figure 2). Major Jurassic structures include the King Salmon, Nahlin, Wann River, and Llewellyn faults in northern British Columbia (Currie & Parrish, 1993; Gabrielse, 1998; Mihalynuk et al., 1999), and the Needlerock, Tadru, and Yukon River faults in Yukon (Figure 3; Colpron et al., 2002, 2003; Colpron & Ryan, 2010; Parsons et al., 2018; Ryan

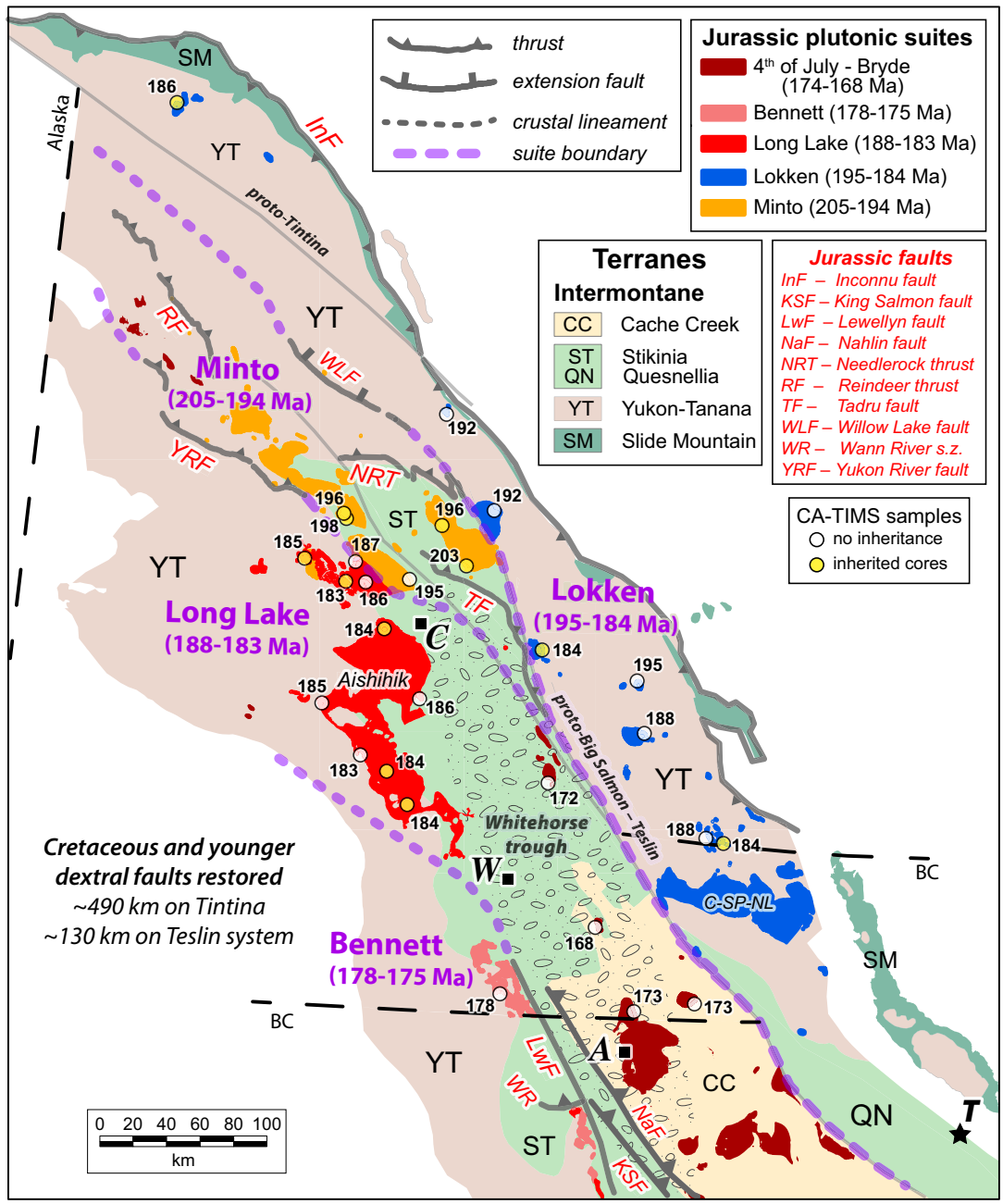

Figure 3. Palinspastic map of Early to Middle Jurassic plutons in southern Yukon and northern British Columbia; after restoration of dextral displacements along the Cenozoic Tintina fault (~490 km) and Cretaceous Big Salmon–Teslin fault system (~130 km; BSTF). Displacement estimates from Gabrielse et al. (2006) and Nelson et al. (2013, p. 88). Restoration on the Tintina fault aligns the portions of the Yukon-Tanana and Slide Mountain terranes northeast of the fault with their counterparts in west-central Yukon. Displacement of the BSTF north of 61°N is inferred to be partitioned into splays of the d'Abbadie, Big Salmon, and Towhata faults (Figure 2), which collectively account for ~125 km of dextral displacement (Nelson & Colpron, 2007; Nelson et al., 2013). Jurassic structures are shown as gray lines with red labels. Dots show the location of samples analyzed by CA-TIMS for this study (Tables 1 and 2 and Appendix 4 in Sack et al., 2020). Ages are rounded for simplicity; see Sack et al. (2020, Tables 1 and 2; Sack et al., 2022) for precise dates. Yellow dots indicate samples for which inherited zircon cores were analyzed by LA-ICPMS. Black star shows approximate location of the Early Jurassic Turnagain complex in northern British Columbia (T; Nixon et al., 2020). Black squares show approximate location of the towns of Atlin (A), Carmacks (C), and Whitehorse (W) for reference. The Aishihik and Coconino-Simpson Peak-Nome Lake (C-SP-NL) batholiths are labeled and discussed in the text.

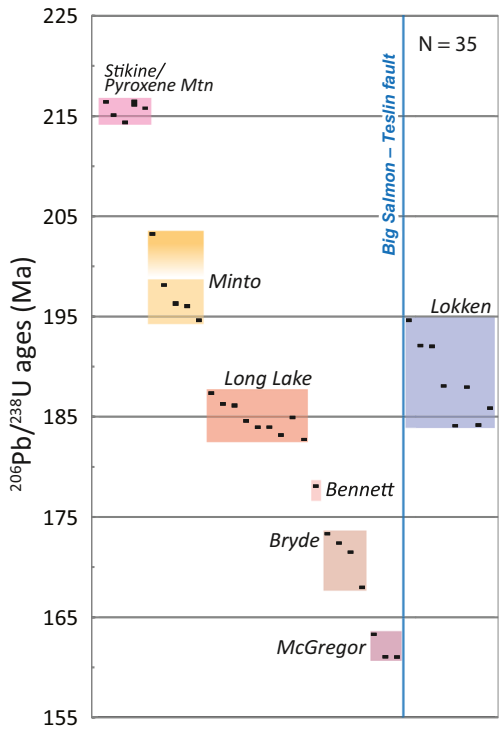

Figure 4. Summary of new CA-TIMS dates constraining the age of Late Triassic and Jurassic plutonic suites in southern Yukon (Tables 1 and 2 and Appendix 4 in Sack et al., 2020; Appendix 2 in Sack et al., 2022). Interpreted ages and their 2σ errors are shown by black boxes. Colored boxes show the range for individual plutonic suites.

et al., 2013, 2014). Metamorphic studies of the Yukon-Tanana terrane in western Yukon and northwestern British Columbia indicate that structural imbrication led to crustal thickening, tectonic burial to depths of 20–30 km, and subsequent exhumation in the Early Jurassic (Berman et al., 2007; Clark, 2017; Dyer, 2020; Gaidies et al., 2021). The Willow Lake fault in central Yukon is a low-angle normal fault inferred to have accommodated part of the Early Jurassic exhumation (Colpron & Ryan, 2010; Knight et al., 2013).

The Intermontane terranes and their Late Triassic to Jurassic plutons are dissected by a series of post-accretionary strike-slip faults, including the Late Cretaceous Teslin, d'Abbadie, Big Salmon, and Towhata faults, and the Paleocene Tintina fault (Figure 2). In seismic and magnetotelluric profiles across southern Yukon (SNORCLE line 3), the Teslin fault appears to be underlain by east-dipping anomalies that project to mid-crustal levels (Cook et al., 2004; Dehkordi et al., 2019). Farther north, in central Yukon, an interpretation of seismic and gravity data across the Intermontane terranes shows the Big Salmon fault as a more significant west-dipping structure that extends to lower crustal levels and is laterally more continuous than the Teslin fault at this latitude (Calvert et al., 2017).

In Figure 3, dextral strike-slip displacement has been restored on major Late Cretaceous and Paleocene faults in order to show the configuration of terranes and distribution of Early and Middle Jurassic plutonic suites in Late Jurassic to Early Cretaceous time, after imbrication of the Intermontane terranes and accretion to western North America. This Early Cretaceous palinspastic map provides the framework for the following discussion of Late Triassic to Jurassic magmatism in the Intermontane terranes of Yukon.

3. Late Triassic-Jurassic Plutonic Suites

Extensive studies, summarized in this article, result in subdivision of the Late Triassic to Jurassic plutons in Yukon into eight plutonic suites based mainly on age (Figure 4) and composition (Figure 5), but also to some extent on relationship with their host terrane, and geographic distribution (Figures 2 and 3; Sack et al., 2020). From oldest to youngest, these suites are:

1. The Late Triassic Pyroxene Mountain (220–214 Ma) and Stikine (217–214 Ma) suites.
2. The latest Triassic to Early Jurassic Minto (205–194 Ma), Lokken (195–184 Ma), Long Lake (188–183 Ma), and Bennett (178–175 Ma) suites.
3. The Middle Jurassic Bryde suite (174–168 Ma) and Late Jurassic McGregor suite (163–146 Ma).

3.1. Methods and Data Set

The core of this data set was acquired during field investigations of 32 plutons between 2014 and 2018, augmented with data collected during previous regional mapping programs (1999–2013; see Sack et al., 2020, for complete sources of data). Of the more than 450 granitoid rock samples collected, 171 were slabbed and stained for petrographic analysis (Appendices 2 and 13 in Sack et al., 2020), including semi-automated estimates of modal abundances of quartz, alkali feldspar, plagioclase, and mafic minerals using the ImageJ software (Figure 5a; Schneider et al., 2012). Thin sections were cut from 209 samples and 204 samples were analyzed for major and trace element geochemistry (Figures 5b–5d; Appendix 8 in Sack et al., 2020). Age ranges for the eight plutonic suites are anchored on 35 high-precision U-Pb zircon dates determined using the chemical abrasion thermal ionization mass spectrometry (CA-TIMS) method (Figure 4; Tables 1 and 2 and Appendix 4 in Sack et al., 2020; see also Sack et al., 2022 for one additional sample). Thirty-four of these samples were analyzed at Boise State University (BSU) and one sample at the University of British Columbia (UBC). Most samples analyzed at BSU were first imaged by cathodoluminescence (CL) and analyzed by laser ablation inductively coupled plasma mass spectrometry (LA-ICPMS) before CA-TIMS analysis (Appendix 3 in Sack et al., 2020). Approximately 30

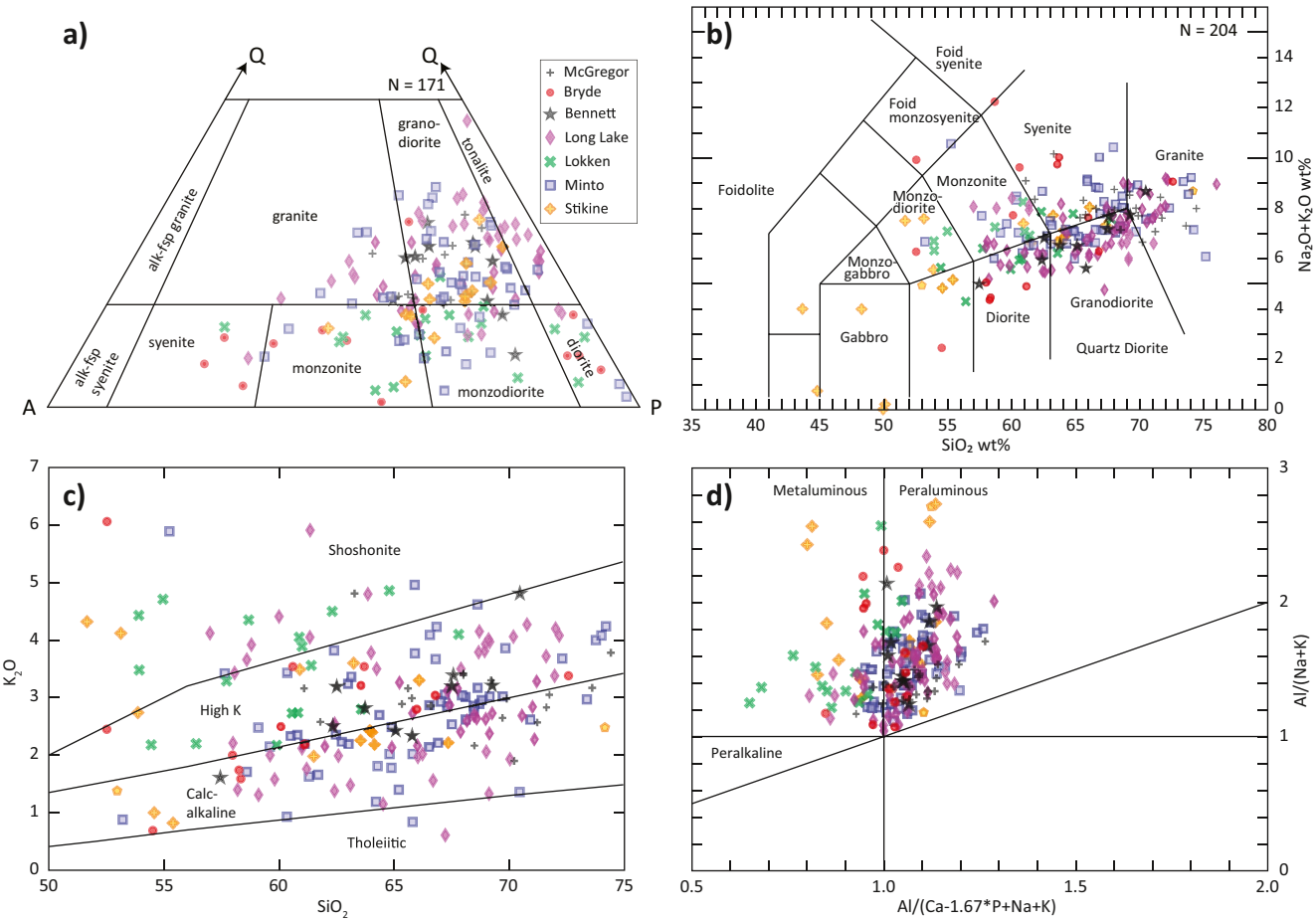

Figure 5. Compositional range of Late Triassic to Jurassic plutonic suites in the Intermontane terranes of Yukon. (a) Simplified Quartz-Alkali-feldspar-Plagioclase plot (after Le Bas & Streckeisen, 1991). (b) Total alkali versus silica diagram for plutonic rocks (after Le Bas et al., 1986). (c) K_2O versus SiO_2 diagram of Peccerillo and Taylor (1976). (d) Alumina saturation index of Shand (1943). Modal abundances from stained hand sample slabs and major element geochemistry from Sack et al. (2020, Appendix 8).

LA-ICPMS spots in each sample were analyzed for U-Pb isotopes and trace element chemistry to characterize the zircon population(s) present. Zircon grains dated by CA-TIMS were selected from the youngest statistically coherent LA-ICPMS population with similar chemical composition and CL response. Inherited cores were encountered in 15 of the 33 samples analyzed and documented by LA-ICPMS (Tables 1 and 2 and Appendix 3 in Sack et al., 2020). The Atlas also reports new $^{40}Ar/^{39}Ar$ dates for hornblende, muscovite, and biotite from 25 samples (Appendix 6 in Sack et al., 2020). Most of the mica dates provide estimates for cooling of these plutons to upper crustal levels (≤300°C–350°C; Hodges, 2014). A few hornblende dates from Late Triassic intrusions and muscovite dates in the central part of the Late Jurassic McGregor pluton provide the best estimate for crystallization for these plutons.

Whole rock analyses of Rb-Sr and Sm-Nd isotopes were acquired at Carleton University from 30 of the dated samples (Tables 1–4 and Appendix 9 in Sack et al., 2020). Zircons from 22 of the samples dated at BSU were also analyzed for Lu-Hf isotopes using the LA-ICPMS laboratory at Memorial University of Newfoundland (MUN; Appendix 10 in Sack et al., 2020). The Hf isotope data were acquired at MUN on the same zircon mounts used at BSU with 40 μm Hf spot analyses located on top of smaller U-Pb ablation pits so the data are as related as possible.

Crystallization pressures were calculated using the Al-in-hornblende geobarometer for 26 samples that contain the required mineral assemblage (Anderson & Smith, 1995; Hammarstrom & Zen, 1986). Electron microprobe analyses of plagioclase and hornblende were performed at UBC (Tables 1–3 and Appendix 5 in Sack et al., 2020).

Total 1σ errors in pressure generally range from 0.8 to 1.1 kbar, such that all depth estimates quoted in this study have an associated error of ~3 to 4 km.

3.2. Late Triassic Plutonic Suites

Late Triassic plutons associated with arc volcanic rocks of Stikinia occur in two main clusters in southern Yukon. South of Whitehorse (Figure 2), the Stikine suite (217–214 Ma) comprises small monzodiorite, monzonite, and granodiorite plutons (Figure 5a) that intrude Upper Triassic volcanic and volcaniclastic rocks of Stikinia (Lewes River Group) near its western edge. Uranium-lead zircon CA-TIMS $^{206}Pb/^{238}U$ dates range from 216.48 ± 0.06 to 214.42 ± 0.07 Ma (Figure 4). The plutons are oxidized, calc-alkaline to high-K calc-alkaline, and mostly metaluminous (Figures 5c and 5d). They are isotopically juvenile with εNd_t of +5.2 to +5.3 and $^{87}Sr/^{86}Sr_i$ of 0.7042 to 0.7047 (Figures 6 and 7). Zircons from the Stikine suite have εHf_t ranging +9.7 to +11.6 (Figure 6c). No inherited zircon cores were encountered in the Stikine suite. Crystallization pressure estimates were determined from only one pluton (Friday Creek, Figure 2) and indicate emplacement at 3.1–3.5 kbar (emplacement depths of 12–13 km; Figure 8).

A second cluster of small Late Triassic plutons north of Carmacks (Figure 2), the Pyroxene Mountain suite (220–214 Ma; Ryan et al., 2013), is not as well studied. They include mainly hornblende gabbro, diorite, and pyroxenite that are generally coarse to very coarse grained. The plutons intrude metamorphic rocks of the Yukon-Tanana terrane northwest of the last exposures of Upper Triassic volcanic rocks of Stikinia (Povoas Formation, Lewes River Group) with which the plutons are inferred to be comagmatic (Ryan et al., 2013; Tempelman-Kluit, 1984, 2009). Similar coarse grained hornblende gabbro and amphibolite also occur within rafts in Early Jurassic plutons of the Minto suite where they intrude Upper Triassic metavolcanic rocks (Ryan et al., 2013). Zircons from plutons of the Pyroxene Mountain suite previously yielded imprecise U/Pb dates between 220 and 211 Ma, but $^{40}Ar/^{39}Ar$ dates from hornblende of the Pyroxene Mountain pluton and amphibolite rafts in Early Jurassic batholiths have a narrower range from 218 to 214 Ma (Sack et al., 2020). A new CA-TIMS date from a Pyroxene Mountain pluton at Mount Nansen, west of Carmacks (Figure 2; previously dated at ca. 211 Ma by LA-ICPMS; Klöcking et al., 2016), has an age of 216.16 ± 0.07 Ma (Sack et al., 2022) and CA-TIMS analysis of zircon fragments in a mineralized raft at the Carmacks Copper deposit indicate a protolith age of 217.53 ± 0.16 Ma (Kovacs et al., 2020). These results suggest that the Pyroxene Mountain suite is the northern extension of the Stikine suite in central Yukon and that Stikinia is locally anchored on the Yukon-Tanana terrane.

3.3. Early Jurassic Plutonic Suites

Early Jurassic granitoid plutons are widespread in southern Yukon, where they occur on either side of Triassic volcanic rocks of Stikinia/Quesnellia, and Jurassic sedimentary strata of the WT (Figures 2 and 3). Although the earliest phases in some plutons of the Minto suite are latest Triassic (ca. 205-203 Ma), the bulk of these plutons are Early Jurassic (198–195 Ma) and assigned to that epoch here for simplicity. The Early Jurassic plutons have a distinct character on either side of the Big Salmon-Teslin fault system (BSTF). West of the BSTF, large batholiths of the Minto (205–194 Ma), Long Lake (188–183 Ma), and Bennett (178–175 Ma) suites intrude the boundary between Stikinia and Yukon-Tanana terranes. They are mainly composed of granodiorite and granite (Figures 5a and 5b) with the older Minto suite intruding near the apex of Late Triassic Stikinia and progressively younger batholiths of the Long Lake and Bennett suites intruding its western edge to the south (Figures 3 and 4). East of the BSTF, Early Jurassic plutons of the Lokken suite (195–184 Ma) are distinctly more mafic and alkalic (Figures 5a and 5b), typically form small plutons, show no systematic age distribution (Figures 3 and 4), and intrude only the Yukon-Tanana terrane.

3.3.1. Minto Suite

The Minto suite is predominantly composed of hornblende-biotite granodiorite and subordinate granite, quartz monzonite, and diorite (Figures 5a and 5b). Uranium-lead zircon CA-TIMS $^{206}Pb/^{238}U$ dates range mainly from 198.22 ± 0.06 to 194.71 ± 0.07 Ma (Figure 4). The granodiorite is medium grained equigranular to coarse grained and K-feldspar porphyritic. It is locally foliated or gneissic, but more typically unfoliated. Euhedral magmatic epidote is common in granodiorite of the Minto suite (Sack et al., 2020). Minto suite plutons are

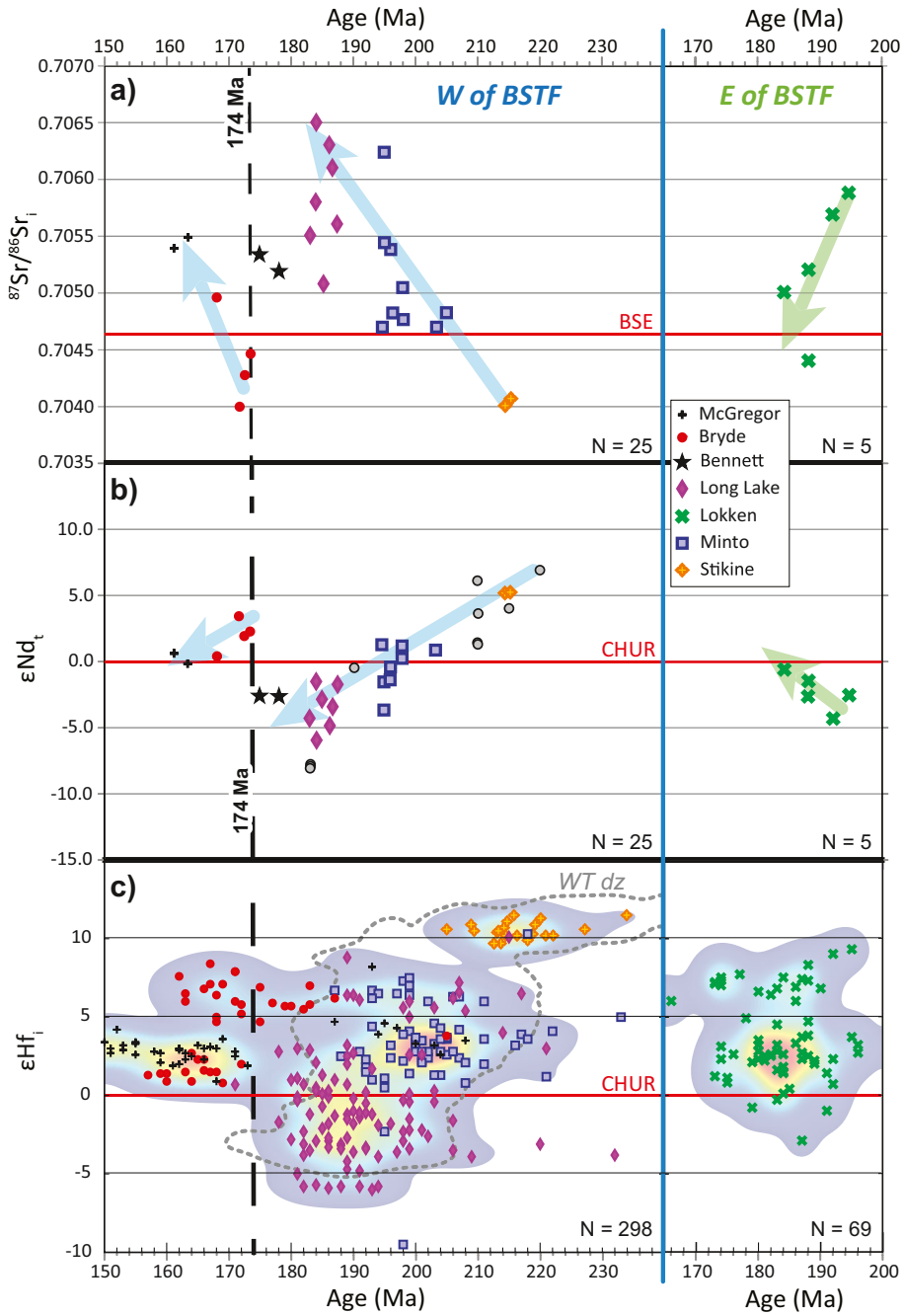

Figure 6. Plots of $^{87}Sr/^{86}Sr_i$ (a), εNd_t (b), and zircon εHf_t (c) versus age for Late Triassic to Jurassic plutons in southern Yukon. Note the contrasting isotopic evolution from plutons west and east of the Big Salmon-Teslin fault system. Data from Sack et al. (2020, Tables 1–4, Appendices 9 and 10). Whole rock Sr (a) and Nd (b) analyses were done on samples precisely dated by CA-TIMS while the Hf data in c was acquired by LA-ICPMS spot analyses of igneous zircons yielding a scatter of U-Pb dates. Gray circles in (b) are from volcanic and sedimentary rocks of the Stuhini and Laberge groups reported in Jackson et al. (1991). Note that the age of sandstone samples with subchondritic εNd_t were corrected using detrital zircon maximum depositional ages from nearby strata of the Laberge Group (Kellett & Iraheta Muniz, 2019). Contours for Hf isotopic data in (c) were generated using the HafniumPlotter routine of Sundell et al. (2019). Dash gray line shows the 95th percentile contour for detrital zircon from the Laberge Group (WT dz; van Drecht, 2019; $n = 954$). *Abbreviations*. BSE, bulk silicate Earth; CHUR, chondritic uniform reservoir.

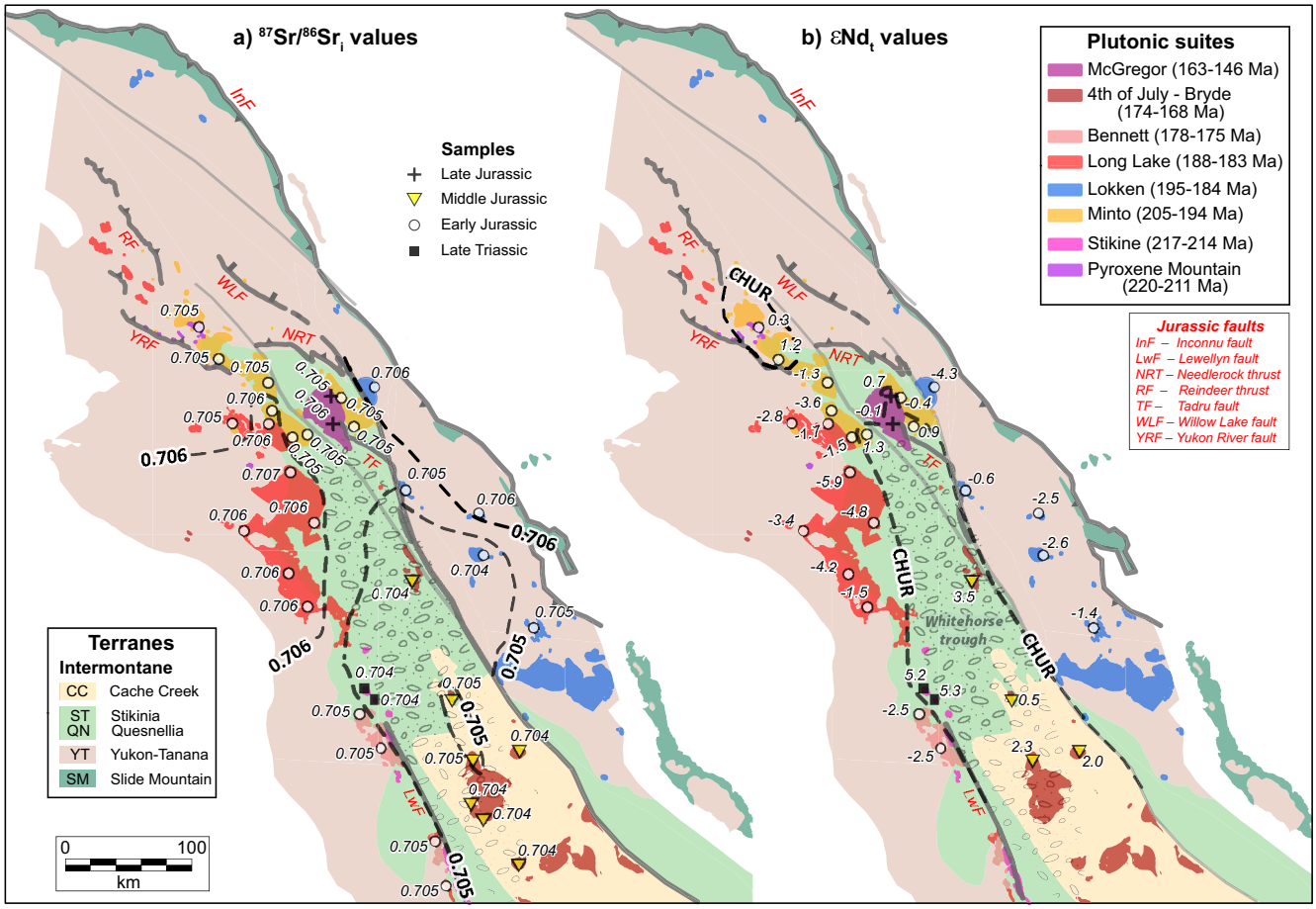

Figure 7. Distribution of $^{87}Sr/^{86}Sr_i$ (a) and εNd_t (b) values for Late Triassic and Jurassic plutons shown on palinspastic map from Figure 3. Isotopic data from Sack et al. (2020, Tables 1–4). Data for the southernmost Sr samples in (a) are from Currie (1994) for Early Jurassic plutons (Bennett suite; $n = 2$) and Mihalynuk et al. (1992) for the Middle Jurassic Fourth of July suite ($n = 3$).

generally oxidized, calc-alkaline to high-K calc-alkaline to weakly shoshonitic, and predominantly peraluminous (Figure 5). Whole rock isotopic data range from −3.6 to +1.3 for εNd_t, and 0.7047–0.7062 for $^{87}Sr/^{86}Sr_i$; εHf_t in zircon range from +0.5 to +10.9 (Figures 6 and 7).

The K-feldspar megacrystic border phase of the Tatchun batholith yielded an older CA-TIMS $^{206}Pb/^{238}U$ date of 203.32 ± 0.06 Ma (Figure 4). Although this is the only precisely dated latest Triassic phase in this study, the presence of 205–203 Ma zircon antecrysts in the Granite Mountain batholith (Kovacs et al., 2020; Sack et al., 2020) and an imprecise date of 204.9 ± 3.3 Ma from the Pelly pluton (Knight et al., 2013) suggest that this early phase may be more widespread than presently documented in the Minto suite. Inherited zircons are documented in the Granite Mountain, Minto, and Tatchun plutons (Figure 3; Kovacs et al., 2020; Sack et al., 2020). They show a bimodal age distribution with peaks in the Late Triassic (ca. 213 Ma) and Mississippian (ca. 344–327 Ma; Figure 9a). Late Triassic zircons have εHf_t of +3.2 to +6.0 and Mississippian zircons have εHf_t of +3.7 to +10.9.

Crystallization pressure estimates using the Al-in-hornblende method were determined for the Granite Mountain, Minto, Walhalla, and Tatchun plutons (McCausland et al., 2002; Sack et al., 2020; Tafti, 2005; Topham et al., 2016). Plutons west of the Teslin fault have emplacement pressures of 4.8–5.9 kbar, whereas samples from the Tatchun batholith to the east of the fault consistently yield higher pressures of 6.4–6.8 kbar (Figure 8). These values suggest emplacement depths of 15–25 km for the Granite Mountain, Minto, and Walhalla plutons, and of 21–30 km for the Tatchun batholith. These emplacement pressures are consistent with upper greenschist to amphibolite facies metamorphism of host rocks for these plutons (Read et al., 1991).

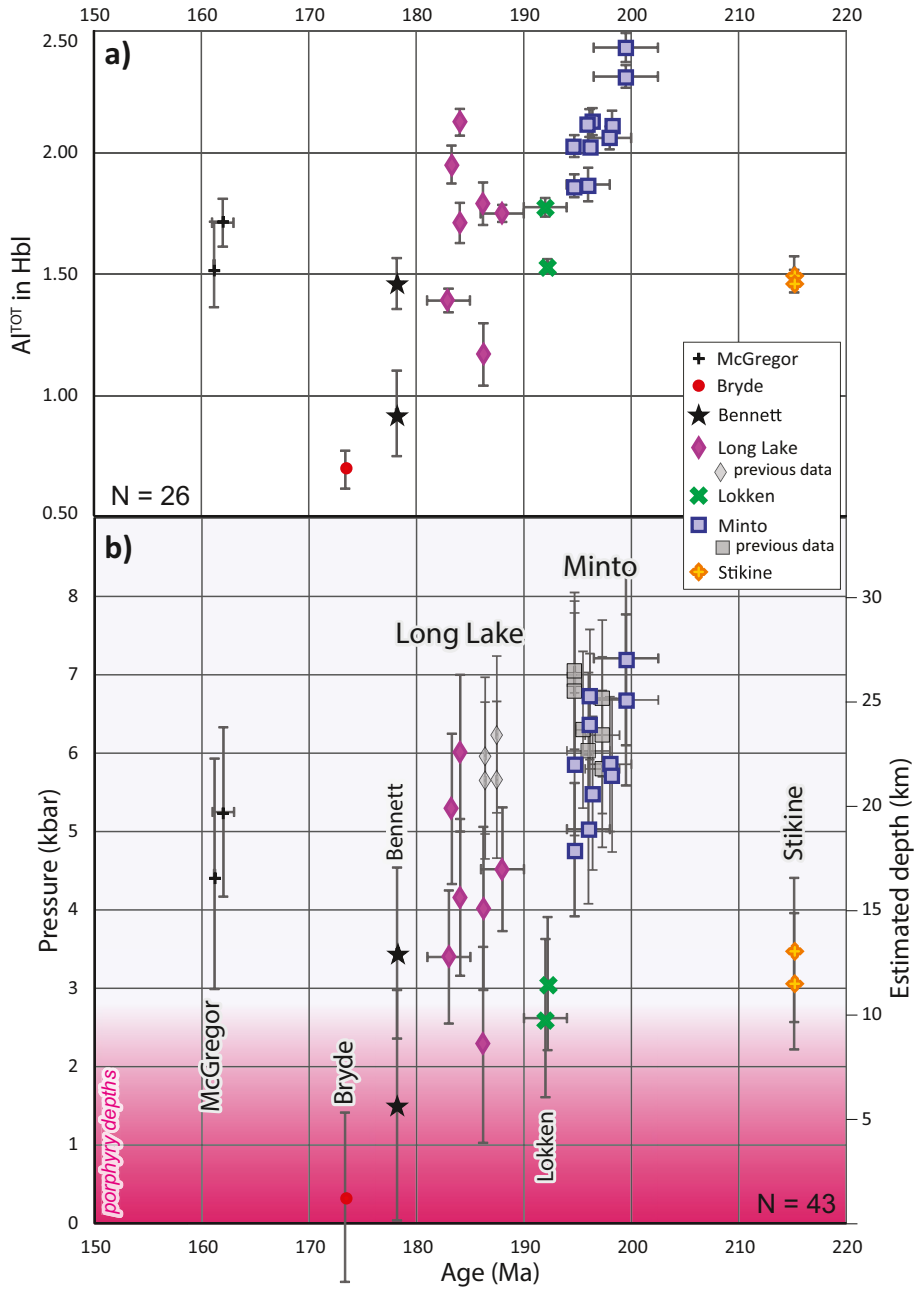

Figure 8. Plot of total Al content (Al_{TOT}) of hornblende (a) and Pressure (b) versus age for Late Triassic and Jurassic plutons in Yukon. Pressures calculated using the Al-in-hornblende geobarometer of Anderson and Smith (1995). Data is presented in Sack et al. (2020, Tables 1–3 and Appendix 5). Depth estimated using a lithostatic gradient of ~3.7 km/kbar. Samples from previous studies are shown in gray; data from McCausland et al. (2002) and Tafti (2005).

Plutons of the Minto suite contain a belt of Cu-Ag-Au deposits (Minto, Carmacks Copper and Stu; Figure 2). The mineralization is dated at ca. 217–213 Ma and occurs in variably metamorphosed and migmatized rafts and xenoliths of foliated intermediate to mafic meta-igneous rocks of probable Stikine suite affinity, enveloped within massive plutonic phases of the Minto suite (Kovacs et al., 2020; Sack et al., 2020).

3.3.2. Long Lake Suite

The Long Lake suite is primarily represented by the Aishihik batholith, Big Creek pluton, and southwest portion of the Granite Mountain batholith (Figures 2 and 3); it ranges from tonalite-granodiorite to granite and syenite (Figures 5a

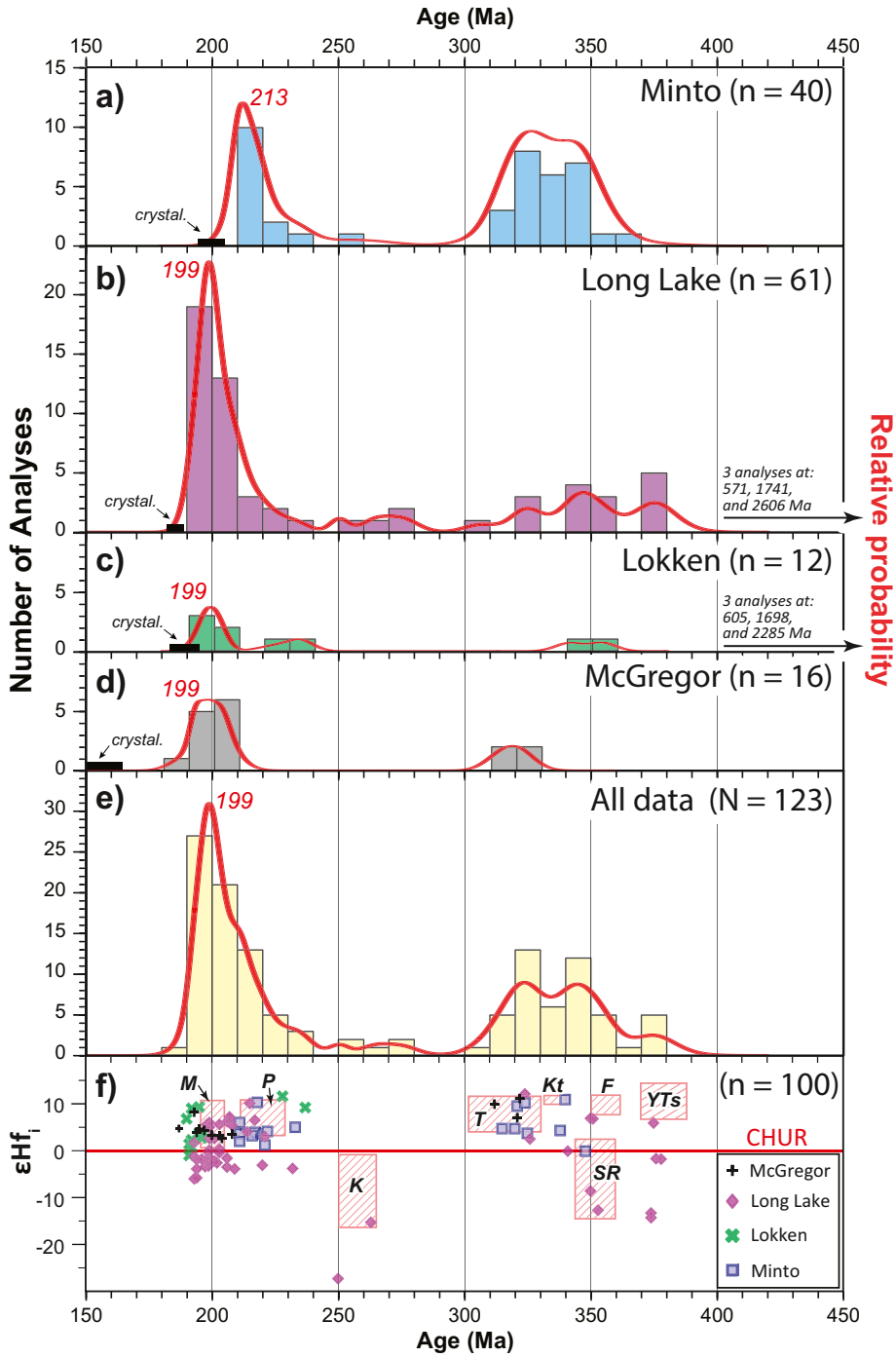

Figure 9. Probability density plots for Phanerozoic dates and εHf_t data from inherited zircon cores analyzed by LA-ICPMS (Appendices 3 and 10 in Sack et al., 2020). (a) Minto suite; (b) Long Lake suite; (c) Lokken suite; (d) McGregor suite; and (e) composite plot for all analyses. The range of crystallization age (crystal.) from CA-TIMS dates for each suite (Figure 4) is indicated by black bar at the young end of the age spectra. (f) Plot of εHf_t versus age for inherited zircon cores. Hatched, pink areas indicate ranges of εHf_t values for source units from the literature (or equivalent range for εNd_t data, calculated using equation of Vervoot et al., 1999). *Abbreviations*. F, Finlayson assemblage, mafic rocks εNd_t (Creaser, Erdmer, et al., 1997; Piercey et al., 2006); K, Klondike assemblage, felsic rocks εNd_t (Ruks et al., 2006); Kt, Klinkit assemblage, mafic rocks εNd_t (Simard et al., 2003); M, Minto suite, zircon εHf_t (Sack et al., 2020; this study); P, Povoas formation, mafic rocks εHf_t (Bordet et al., 2019); SR, Simpson Range suite, granitoid rocks εNd_t (Piercey et al., 2006); YTs, Devonian detrital zircon εHf_t from Yukon-Tanana terrane of southeastern Alaska (Pecha et al., 2016).

and 5b). The Aishihik batholith comprises two main phases that are close in age and locally intermixed. The older phase is composed of hornblende (±biotite) granodiorite to tonalite. It is fine to medium grained, equigranular to locally K-feldspar porphyritic, and melanocratic with hornblende typically more abundant than biotite. The younger phase comprises coarser grained granodiorite and granite characterized by coarse, gray quartz glomerocrysts. The rock is equigranular to K-feldspar porphyritic, generally leucocratic with mainly biotite and rare hornblende, and local muscovite. Granite phases are commonly associated with aplite dikes and pegmatite pods. The southwest portion of the Granite Mountain batholith is composed mainly of granodiorite and minor granite. Distinctive very coarse grained, hornblende-K-feldspar monzonite and syenite comprise the main phase in the Big Creek pluton.

Zircon CA-TIMS $^{206}Pb/^{238}U$ dates range from 187.46 ± 0.07 to 182.83 ± 0.05 Ma (Figure 4). In the Aishihik batholith, the "older," melanocratic granodiorite phase (Aishihik 1 in Tables 1 and 2 of Sack et al., 2020) yielded dates ranging from 186.22 ± 0.10 to 183.28 ± 0.07 Ma, while the "younger" granite phase (Aishihik 2) is dated at 184.06 ± 0.06 Ma, consistent with intermingling of these phases observed in outcrop.

Granodiorite and granite of the Long Lake suite are oxidized, calc-alkaline to high-K calc-alkaline, and mainly peraluminous, whereas syenite of the Big Creek pluton is oxidized, high-K calc-alkaline to shoshonitic, and metaluminous (Figure 5). Plutons of the Long Lake suite have the most evolved isotopic signature of all Jurassic intrusions in Yukon with $^{87}Sr/^{86}Sr_i$ of 0.7051 to 0.7065, εNd_t of −5.9 to −1.5, and εHf_t in zircon of −5.8 to +6.4 (Figures 6 and 7).

Inherited zircon cores were documented in 7 of the 10 samples analyzed from plutons of the Long Lake suite. The dominant population (53% of analyses) includes cores with dates ranging from 209 to 193 Ma that define a sharp peak at ca. 199 Ma (Figure 9b). Older zircon cores are present but form more subdued populations compared to those in the Minto suite. Six cores yielded Late Triassic dates (233–213 Ma), four are Permian (275–250 Ma), ten are Mississippian (353–324 Ma), and five are Late Devonian (378–374 Ma; Figure 9b). The latest Triassic to Early Jurassic zircons have εHf_t of −6.0 to +7.2, the Late Triassic zircons εHf_t of +3.0 to +10.1, the Permian zircons εHf_t of −15.3, and Devonian-Mississippian zircons εHf_t of −14.3 to +12.1.

Aluminum-in-hornblende pressures were calculated for seven samples from the Aishihik batholith (Figure 2) and range from 2.3 to 6.0 kbar, indicating emplacement depths of 9–23 km (Figure 8; Sack et al., 2020). Previous Al-in-hornblende pressures for the southwest Granite Mountain batholith range from 4.4 to 4.7 kbar (McCausland et al., 2002).

3.3.3. Bennett Suite

The Bennett suite includes much of the Bennett and Alligator Lake plutons south of Whitehorse in Yukon (Figure 2); a trend of plutons from this suite extends into northern British Columbia west of Atlin (Figure 3; Mihalynuk et al., 1999). The Bennett suite is composed of K-feldspar porphyritic granodiorite and equigranular monzodiorite and diorite that are locally weakly foliated (Figure 5a). The groundmass in the granodiorite is generally fine grained with granophyric or graphic textures, suggesting emplacement at shallow depth and/or a water-saturated magma (Sack et al., 2020). A sample of the Bennett Lake batholith has a CA-TIMS $^{206}Pb/^{238}U$ date of 178.18 ± 0.06 Ma (Figure 4). Previous dates from the Bennett suite suggest it may range as young as ca. 175 Ma (Hart, 1995). The rocks are oxidized, subalkaline diorite to granite in composition (SiO_2 62%–70%; Figure 5b). They are calc-alkaline to high-K calc-alkaline and peraluminous (Figures 5c and 5d) and have some of the most enriched trace element concentrations of all Early Jurassic plutons (Sack et al., 2020). Two samples from the Bennett suite have moderately evolved isotopic signatures with $^{87}Sr/^{86}Sr_i$ of 0.7052 and 0.7053, and εNd_t of −2.5 (Figures 6 and 7). No inheritance was documented in the limited LA-ICPMS U-Pb analyses from the Bennett suite. Two samples were analyzed for Al-in-hornblende barometry. One sample has total Al (Al^{TOT}) too low to yield meaningful results, while a crystallization pressure of 3.5 kbar from the other sample suggests emplacement at depths ≤13 km (Figure 8).

3.3.4. Lokken Suite

The Lokken suite is a belt of small plutons intruding metamorphic rocks of the Yukon-Tanana terrane east of the BSTF in southern Yukon (Figures 2 and 3). The Lokken suite extends south into northernmost British Columbia, where it forms parts of the large, composite Coconino-Simpson Peak-Nome Lake batholith (Figure 3; Cui et al., 2017; Han et al., 2020; Roots et al., 2006). The plutons are composed mainly of mesocratic, medium grained,

equigranular hornblende-biotite-clinopyroxene monzodiorite, monzonite, diorite, and granodiorite (Figures 5a and 5b). Zircon CA-TIMS $^{206}Pb/^{238}U$ dates range from 194.67 ± 0.05 to 184.21 ± 0.05 Ma (Figure 4). K-feldspar porphyritic monzonite and granodiorite also occur in some of the younger plutons (e.g., ca. 188–184 Ma Logjam and Two Ladder plutons). Mafic to ultramafic gabbro, pyroxenite, and variably serpentinized dunite locally occur as border phases in some plutons (e.g., Roots et al., 2004). Hornblende-clinopyroxene syenite is present in plutons intruding the Yukon-Tanana terrane northeast of the Tintina fault (e.g., Banana pluton, Figures 2 and 3). Older phases of the Lokken suite are locally foliated and local development of myrmekitic texture suggests subsolidus metasomatism and/or deformation.

Plutons of the Lokken suite are oxidized, subalkaline to alkaline, high-K calc-alkaline to shoshonitic, and metaluminous, and occupy fields distinct from other suites on Figure 5. They have whole rock isotopic data ranging from 0.7044 to 0.7059 for $^{87}Sr/^{86}Sr_i$ and −4.3 to −0.6 for εNd_t; εHf_t in zircon range from −2.9 to +9.3 (Figures 6 and 7). Inherited zircon cores were documented in 3 samples from the youngest part of the Lokken suite (<186 Ma; Figure 3). Only 12 analyses were acquired from these samples (Figure 9c), of which 5 have dates ranging ca. 202–196 Ma, 2 are Late Triassic (ca. 235 and 226 Ma), and 2 are Mississippian (ca. 354 and 341 Ma). Precambrian cores ($n = 3$) with dates of ca. 2,285, 1,698, and 605 Ma were analyzed from the two youngest plutons in the suite, the ca. 184 Ma Logjam and Sawtooth plutons (Figures 2 and 3). Inherited cores with Late Triassic dates have εHf_t of +9.2 and +11.6 (Figure 9).

Only two samples of the Lokken suite had the suitable assemblage for Al-in-hornblende geobarometry. The ca. 192 Ma Lokken and Macmillan Range plutons have calculated pressures of 3.1 and 2.6 kbar, respectively, indicating emplacement at depths of ∼10 to 12 km (Figure 8).

3.4. Middle to Late Jurassic Plutonic Suites

The Middle Jurassic Bryde suite occurs along the central axis of the Intermontane terranes, immediately west of the BSTF, and in between the two main belts of Early Jurassic plutons (Figures 2 and 3). Plutons of the Bryde suite are relatively sparse in southern Yukon but form large batholiths in northern British Columbia, where they are assigned to the Fourth of July suite (Figures 2 and 3; Mihalynuk et al., 1999). They intrude Stikinia and Cache Creek terranes, and the overlapping Early to Middle Jurassic WT, and postdate the Jurassic southwest-verging structural imbrication of these tectonic elements (Bickerton et al., 2020; Mihalynuk et al., 2004).

Plutons of the Bryde suite are composed of hornblende-clinopyroxene-biotite syenite, monzonite, granodiorite, tonalite, and diorite (Figures 5a and 5b). Zircon CA-TIMS $^{206}Pb/^{238}U$ dates for three of four samples analyzed have a narrow range of 173.44 ± 0.05 to 171.62 ± 0.05 Ma (Figure 4). The Michie pluton, east of Whitehorse, is younger with a date of 168.09 ± 0.05 Ma (Figures 2–4). The rock varies from fine to coarse grained, to porphyritic and locally pegmatitic, and from leucocratic to melanocratic. Plutons of the Bryde suite are generally reduced, subalkaline to alkaline, calc-alkaline to high-K calc-alkaline, and straddle the metaluminous and peraluminous fields (Figure 5). They have relatively juvenile isotopic signatures with $^{87}Sr/^{86}Sr_i$ of 0.7040 to 0.7050, and εNd_t of +0.5 to +3.5 (Figures 6 and 7). Zircon εHf_t form two clusters with samples from the ca. 173 to 172 Ma Teslin Crossing and Fourth of July plutons yielding juvenile εHf_t values of +4.7 to +8.5, whereas the younger, ca. 168 Ma Michie pluton has lower εHf_t values of +0.8 to +4.0 (Figure 6c). No inheritance was documented in the four samples that were analyzed. A single sample from the northern tip of the Fourth of July batholith contained the suitable assemblage for Al-in-hornblende geobarometry. However, the very low Al^{TOT} in this sample precluded calculation of reliable pressure estimate (Figure 8). Harris et al. (2003) reported Al-in-hornblende pressures ≤3.1 kbar from the Fourth of July batholith in northern British Columbia.

A single Late Jurassic pluton, the McGregor batholith, intrudes the Boswell assemblage between the Teslin and Towhata faults (Figure 2). It comprises two phases: (a) an older phase of hornblende-biotite granodiorite and granite and (b) a younger, central phase of two-mica granodiorite and tonalite (Sack et al., 2020). The older granodiorite is medium to coarse grained and commonly K-feldspar porphyritic. Medium grained, equigranular granodiorite is locally present, and a foliation is developed locally along the pluton margins. The two-mica (biotite-muscovite) phase is generally fine to medium grained and equigranular, but also locally K-feldspar porphyritic.

Zircon CA-TIMS $^{206}Pb/^{238}U$ dates for three samples of the early granodiorite phase of the McGregor batholith range from 163.42 ± 0.05 to 161.16 ± 0.05 Ma (Figure 4). Zircon from the younger, central phase of two-mica

granodiorite yielded a scatter of U-Pb LA-ICPMS dates between ca. 172 and 136 Ma, including high-U zircon, which precluded precise estimate of its crystallization age (Sack et al., 2020). A muscovite $^{40}Ar/^{39}Ar$ date of 146.8 ± 0.9 Ma provides a minimum age for the two-mica phase of the McGregor batholith. Both phases are reduced, subalkaline, high-K calc-alkaline and peraluminous (Figure 5). Isotopic data were only collected from the older granodiorite phase of the McGregor batholith. Whole rock $^{87}Sr/^{86}Sr_i$ values for two samples are 0.7055, and εNd_t are −0.1 and + 0.7; εHf_t in zircon range from +0.8 to +4.2 (Figures 6 and 7).

Inherited zircon cores were documented in one sample of ca. 161 Ma granodiorite from the McGregor batholith. Twelve of the sixteen spots analyzed have dates ranging from 208 to 187 Ma, defining a peak at ca. 199 Ma (Figure 9d). The remaining four analyses are Carboniferous with dates of 322–312 Ma. Early Jurassic cores have εHf_t of +3.2 to +4.7 and Mississippian cores have εHf_t of +7.0 to +11.0. Two samples of early granodiorite from the McGregor batholith were analyzed for Al-in-hornblende geobarometry and yielded pressures of 4.5 and 5.3 kbar (emplacement depths of ∼17 to 20 km; Figure 8).

4. Magmatic Evolution and Tectonic Settings

The Late Triassic to Jurassic plutons in south-central Yukon were intruded during progressive arc-continent collision and accretion of the Intermontane terranes in the early Mesozoic; they record distinct steps in the transition from arc to syn- and post collisional magmatism.

4.1. Late Triassic Stikine-Lewes River Arc

The Late Triassic (ca. 217–214 Ma) plutons of the Stikine suite intrude comagmatic, Upper Triassic (Carnian-Norian) volcanic and volcaniclastic rocks of the Povoas formation (Lewes River Group, Stikinia) in southern Yukon (Figure 2). Stikine suite rocks have metaluminous, calc-alkaline compositions and juvenile isotopic signatures (average εNd_t +5.3; εHf_t in zircon of +10.0; Figure 6) that are consistent with the primitive arc tholeiite to calc-alkaline basalt compositions of the Povoas formation (average εNd_t +7.5; εHf_t +7.3; Bordet et al., 2019). These data support correlation with the Stuhini-Takla groups and related Late Triassic plutons in British Columbia (average εNd_t +7.5; Dostal et al., 1999), and the concept that these formed parts of a continuous Late Triassic arc system (e.g., Dostal et al., 1999; Mihalynuk et al., 1994, 1999). The Late Triassic gabbro and pyroxenite of the Pyroxene Mountain suite (best ages ca. 218–214 Ma) are the northern extension of the Stikine suite in central Yukon (Figure 2; Ryan et al., 2013; Tempelman-Kluit, 1984, 2009). The Pyroxene Mountain suite intrudes the Yukon-Tanana terrane north of Carmacks, suggesting that the northern end of the Late Triassic arc of Stikinia was locally anchored on Yukon-Tanana basement. The ca. 215–212 Ma Taylor Mountain batholith and related plutons of east-central Alaska also intrude the Yukon-Tanana terrane and likely represent the northernmost expression of Stikine arc magmatism (Figure 1; Dusel-Bacon et al., 2015).

4.2. Early Jurassic Syn-Collisional Magmatism

The style of magmatism in the northern Intermontane terranes of Yukon changed profoundly in the latest Triassic to Early Jurassic, from juvenile intra-oceanic arc to a spatial-temporal sequence of syn-collisional pluton clusters. These plutons were intruded after crustal thickening and burial of the Yukon-Tanana terrane was initiated at ca. 205–200 Ma (Clark, 2017; Kovacs et al., 2020) and during the following phase of exhumation recorded along the flanks of the WT. Crustal thickening was accommodated along a series of southwest-verging shear zones and thrust faults, of which the Needlerock, Tadru, Yukon River, and Reindeer faults are inferred remnants (Figure 3; Colpron et al., 2002, 2003; Parsons et al., 2018; Ryan et al., 2013, 2014). This latest Triassic to Early Jurassic orogenic activity is inferred to record the initiation of the northern Cordilleran orogen (Colpron et al., 2015).

4.2.1. West of the BSTF

Plutons intruding Stikinia and Yukon-Tanana terranes west of the BSTF form large batholiths of generally peraluminous, calc-alkaline to shoshonitic compositions with more evolved isotopic signatures (εNd_t −5.9 to +1.3; zircon εHf_t −6.0 to +10.3; Figure 6). In southern Yukon, the locus of magmatism migrated southward through the Early Jurassic, with the older Minto suite (ca. 205–194 Ma) in the north and progressively younger plutons of the Long Lake (ca. 188–183 Ma) and Bennett suites (ca. 178–175 Ma) to the south (Figures 3 and 4). Early

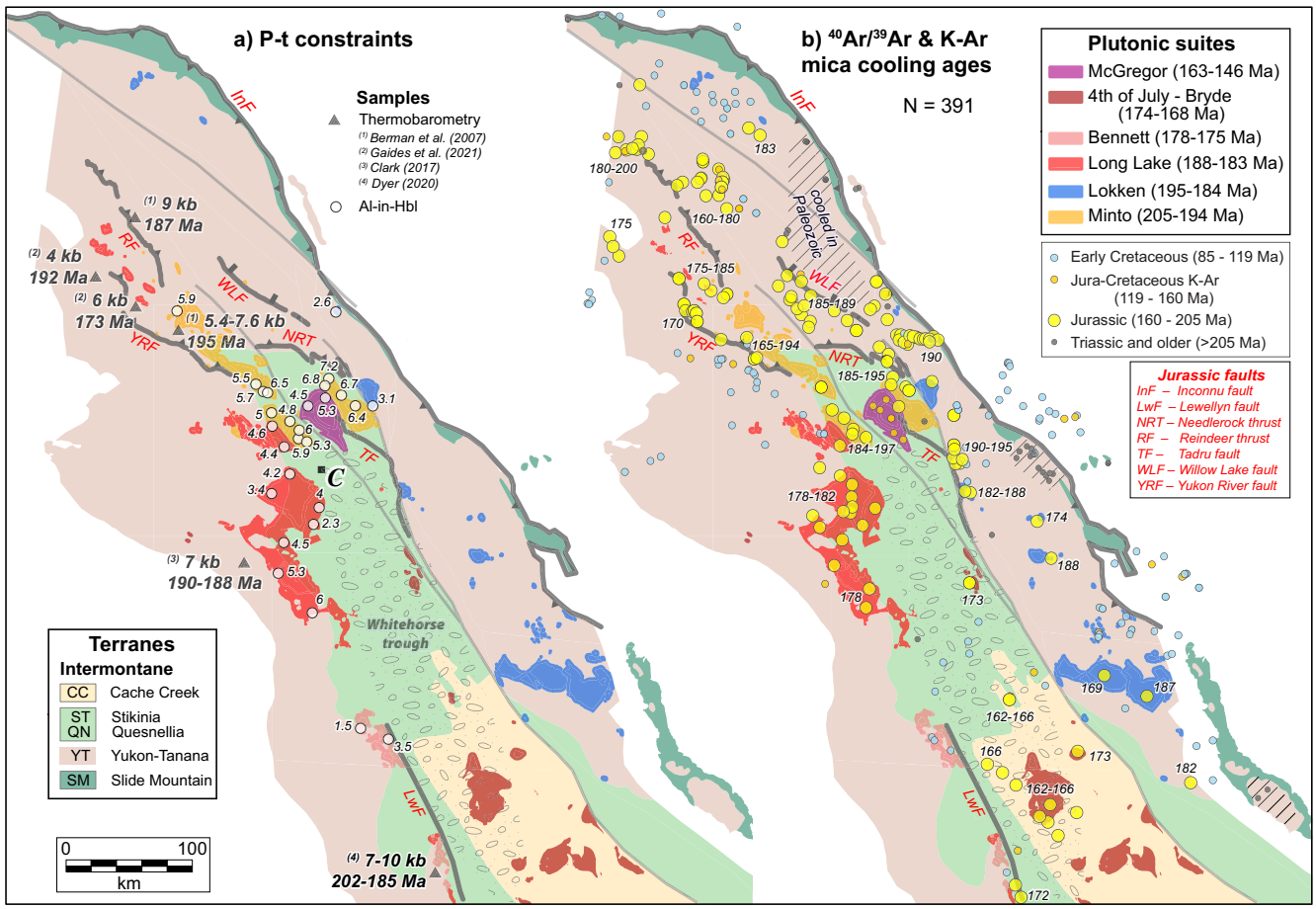

Figure 10. (a) Spatial distribution of crystallization pressure estimates from Al-in-hornblende geobarometry in Jurassic granitoid plutons (data from Tables 1–3 in Sack et al., 2020) and Early Jurassic peak pressures from regional metamorphic studies of the Yukon-Tanana terrane (Berman et al., 2007; Clark, 2017; Dyer, 2020; Gaidies et al., 2021). (b) Mica cooling ages for metamorphic and igneous rocks of the Intermontane terranes in Yukon (data from compilation of the Yukon Geological Survey, 2020c) and northern British Columbia (data from compilation of Han et al., 2020). Jurassic cooling ages are highlighted by yellow circles with labels showing the range for cluster of ages. Hatched area in the hanging wall of the Willow Lake fault (WLF) indicates part of the Yukon-Tanana terrane that cooled in the Paleozoic (Colpron et al., 2015; Knight et al., 2013; Staples et al., 2016). Sample locations are shown on the palinspastic restoration from Figure 3. *Abbreviation*. C, Carmacks.

Jurassic plutons west of the BSTF also show progressively more evolved isotopic signatures through time, with the Minto suite yielding near chronditic εNd_t (average of −0.4) compositions and the younger Long Lake and Bennett suites having more evolved εNd_t averages of −3.5 and −2.5, respectively (Figure 6b). Similar patterns are apparent in $^{87}Sr/^{86}Sr_i$ (Figure 6a) and εHf_t in zircon (Figure 6c). This progressive shift to more evolved isotopic signatures indicates an increase in crustal interaction through time. Incorporation of older crustal components (e.g., Snowcap assemblage; Piercey & Colpron, 2009) into the Early Jurassic magma is also reflected in the relative abundance of inherited zircon cores in plutons of the Minto and Long Lake suites (Figures 3 and 9).

Plutons of the Minto suite were emplaced in the mid- to lower crust during peak regional metamorphism, and local development of a solid-state foliation in early phases suggest syn-tectonic intrusion. They have Al-in-hornblende crystallization pressures of ~5 to 7 kbar (~20 to 25 km; Figure 8) that are consistent with the common occurrence of magmatic epidote in these plutons (Sack et al., 2020; Zen & Hammarstrom, 1984). Although the presence of magmatic epidote and the Al-in-hornblende geobarometer have been questioned as reliable indicators for depth of emplacement (see Schmidt & Poli, 2004, for discussion), regional metamorphic studies of the Yukon-Tanana terrane in western Yukon indicate peak pressures in the Early Jurassic (4–9 kbar, ca. 195–188 Ma; Berman et al., 2007; Clark, 2017; Gaidies et al., 2021) that are broadly consistent with Al-in-hornblende pressures from Minto suite plutons (Figure 10a). In particular, kyanite-rich metapelitic rocks in the aureole of the 199.1 ± 6.8 Ma Walhalla pluton (Figure 2) formed at 195.0 ± 1.7 Ma (monazite) and have an estimated pressure of 5.4–7.6 kbar at 600°C (Berman et al., 2007), which is consistent with the Al-in-hornblende pressure estimate of 5.9 ± 0.9 kbar for the

granodiorite in the pluton (Figure 10a). North of Carmacks, Upper Triassic rocks of Stikinia are locally metamorphosed to greenschist and lower amphibolite facies (Colpron et al., 2003; Colpron & Ryan, 2010; Read et al., 1991).

Exhumation of the Minto suite plutons and their Yukon-Tanana host rocks followed shortly after intrusion and peak metamorphism (Clark, 2017), and ca. 200–180 Ma mica dates suggest cooling below 300°C–350°C in the Early Jurassic (Figure 10b). The Minto and Granite Mountain plutons were emplaced at ~20 km at ca. 198–195 Ma and exhumed by ≤10 km in 8–14 Myr, for average exhumation rates of 0.7–1.3 mm/yr (Sack et al., 2020). To the east, the Tatchun batholith was emplaced deeper (~25 km) and exhumed ~15 km in only 2–7 Myr, for average exhumation rates of 2.1–7.5 mm/yr. The higher exhumation rates suggest that unroofing may have been aided by tectonic denudation. The Willow Lake fault is a low-angle extension fault that is inferred to have accommodated part of the tectonic denudation in the Early Jurassic (Figures 2 and 3; Colpron & Ryan, 2010). Its hanging wall contains relatively undeformed and unmetamorphosed Mississippian volcanic and plutonic rocks of the Yukon-Tanana terrane that preserve Mississippian mica cooling ages (Joyce et al., 2015; Knight et al., 2013). These rocks formed an upper crustal lid beneath which strongly foliated, locally protomylonitic, amphibolite facies metasedimentary and metaplutonic rocks in the footwall were exhumed in the Early Jurassic (ca. 189-185 Ma mica cooling ages; Figure 10b).

Plutons of the Long Lake (ca. 188–183 Ma) and Bennett suites (ca. 178–175 Ma) were emplaced at shallower crustal levels during this Early Jurassic phase of exhumation (Figures 8 and 10a). Plutons of the Long Lake suite generally yield Al-in-hornblende pressures of 3.4–5.3 kbar (emplacement depths of 13–20 km) and cooled rapidly within 2–4 Myr after crystallization. Similarly, Al-in-hornblende pressures of 4.3–5.5 kbar are reported from Early Jurassic plutons of the Long Lake and Bennett suites in northern British Columbia (Currie, 1994).

4.2.2. East of the BSTF

The Lokken suite (ca. 195–184 Ma) intrudes the Yukon-Tanana terrane east of the BSTF. It comprises mainly small plutons in Yukon but includes the large, composite Coconino-Simpson Peak-Nome Lake batholith in northern British Columbia (Figures 2–4). Unlike the Early Jurassic plutons to the west, there is no apparent pattern of age distribution in the Lokken suite. The Lokken plutons are generally more mafic, locally ultramafic, metaluminous, and high-K calc-alkaline to shoshonitic with subchondritic εNd_t, $^{87}Sr/^{86}Sr_i$ generally >0.7047, and εHf_t in zircon of −2.9 to +9.3 (Figures 6 and 7). Overall, the Lokken suite has a range of isotopic values comparable to Minto suite plutons to the west. In contrast to Early Jurassic plutons west of the BSTF, the Lokken suite shows an apparent trend of decreasing crustal influence through time, with a generally more juvenile isotopic signature in younger plutons (Figure 6). Zircon inheritance is less common in Lokken suite plutons, with inherited cores encountered in only three of eight samples analyzed, and in younger plutons of the suite (ca. 186–184 Ma; Figures 3 and 9). Limited Al-in-hornblende data suggest emplacement depths ≤10 km (Figures 8 and 10a), consistent with predominantly greenschist facies assemblages in the Yukon-Tanana host rocks (Read et al., 1991). Mica dates also suggest relatively rapid cooling within ≤2 Myr (Figure 10b). Local development of foliation and myrmekitic textures suggest emplacement during deformation and metamorphism.

Lokken suite plutons in Yukon are probably along-strike equivalents of syn-tectonic, Alaskan-type intrusions in Quesnellia and Yukon-Tanana terranes in British Columbia, including the Turnagain (Figure 3; ca. 190–185 Ma; Nixon et al., 2020) and Polaris complexes (ca. 186 Ma; Nixon et al., 1997). Like the Turnagain complex, plutons of the Lokken suite locally include mafic to ultramafic phases and were apparently emplaced during regional deformation and metamorphism related with imbrication of Yukon-Tanana and Quesnellia with the western North American margin.

4.3. Middle to Late Jurassic Post-Collisional Magmatism

Middle Jurassic plutons of the Bryde and Fourth of July suites intruded the axis of the Intermontane terranes and the overlapping WT (Figures 2 and 3) after initial imbrication with Stikinia and Cache Creek terranes (Bickerton et al., 2020; Mihalynuk et al., 2004). The post-collisional Bryde suite is generally more alkalic with juvenile $^{87}Sr/^{86}Sr_i$ (<0.7047), and superchronditic εNd_t and zircon εHf_t values (Figure 6) that indicate renewed mantle input in the Middle Jurassic (ca. 174 Ma). By the Late Jurassic, peraluminous granodiorite and granite of the McGregor pluton (ca. 163–146 Ma) show another shift to more evolved isotopic signatures and increasing crustal input. The shift in isotopic values between the Middle and Late Jurassic is similar to the trend observed

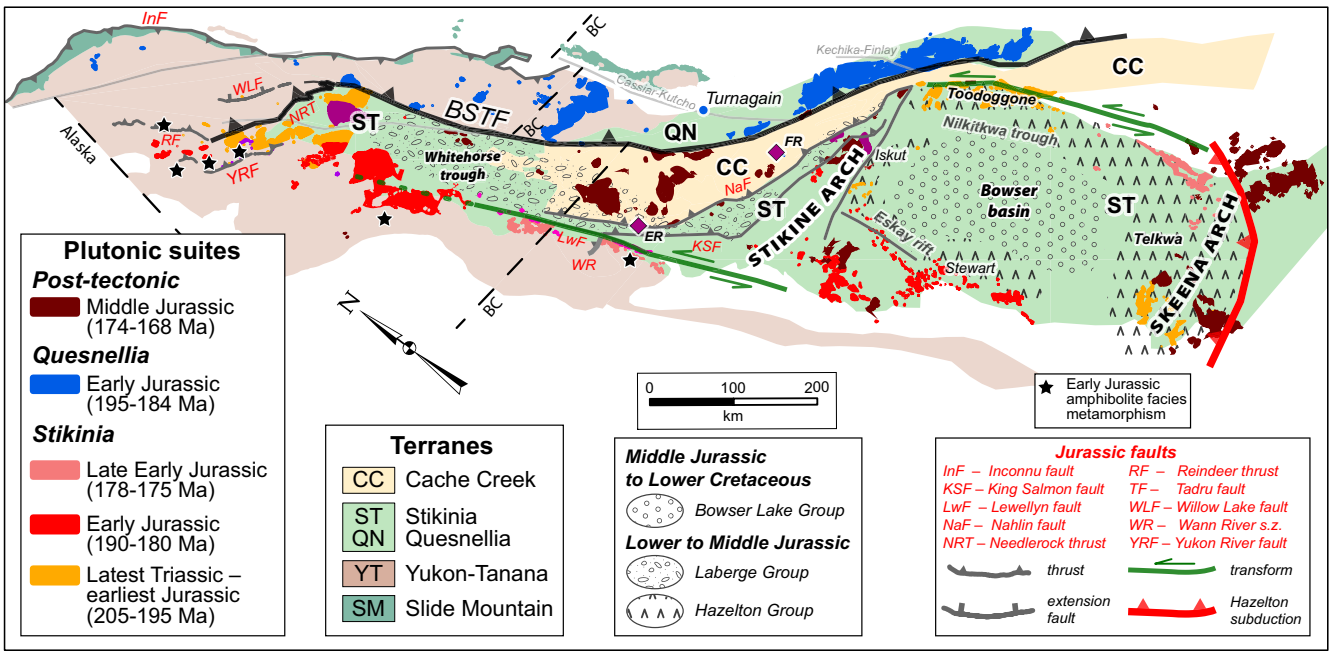

Figure 11. Regional relationships of Early to Middle Jurassic sedimentary basins, volcanic, and magmatic belts in the northern Intermontane terranes of Yukon and northern British Columbia. Palinspastic restoration as in Figure 3 with additional restoration of dextral displacement on the Cassiar-Kutcho (~50 km) and Kechika-Finlay (~195 km) faults following Gabrielse (1985), Evenchick (1988), and Gabrielse et al. (2006). Note that this map is rotated with modern-day north pointing to upper left. Heavy red line along the Skeena arch marks approximate location of the Hazelton subduction zone (teeth pointing to upper plate). Heavy black line with teeth indicates the western boundary of Quesnellia with Cache Creek and Stikinia, which follows the modern traces of the Big Salmon-Teslin fault system (BSTF). Heavy green lines are traces of inferred Early Jurassic sinistral transform faults. Purple diamonds show locations of Early Jurassic eclogite clasts in Laberge Group (Eclogite Ridge, ER) and Middle Jurassic blueschists in the French Range (FR), Cache Creek terrane.

in Late Triassic to Early Jurassic plutons west of the BSTF (Figure 6) and likely reflects continued crustal thickening and growth of the orogen.

4.4. Whitehorse Trough

Crustal thickening and emplacement of Early Jurassic plutons were coincident with development of the WT (Colpron et al., 2015), a marine synorogenic sedimentary basin that overlaps Stikinia and Cache Creek terranes north of the Stikine arch (Figures 1 and 11). Its siliciclastic fill, the Laberge Group, comprises proximal, shallow marine sandstone, and conglomerate along the northern (Tanglefoot formation) and western margins (Takwahoni Formation), and generally more distal, deep-water sandstone-mudstone (turbidite), and mass-flow conglomerate of the Richthofen and Inklin formations near the center of the basin (English et al., 2005; Hart, 1997; Johannson et al., 1997; Lowey, 2008; Souther, 1971; Wheeler, 1961). Subsidence in the WT began in late Hettangian to Sinemurian (ca. 199 Ma) during emplacement of the Minto suite within a thickening orogen and continued through Early Jurassic exhumation until the Bajocian (Middle Jurassic). Pliensbachian (ca. 188–186 Ma) crystal-lithic tuff of the Nordenskiöld facies occur at various stratigraphic levels within the Tanglefoot and Richthofen formations in Yukon and likely represent pyroclastic deposits sourced from magma of the Long Lake suite to the west (Colpron & Friedman, 2008). Conglomerate clasts in the Laberge Group indicate progressive unroofing of Stikinia with mostly volcanic and sedimentary clasts in Sinemurian to lower Pliensbachian strata, mostly plutonic clasts in the upper Pliensbachian, and appearance of metamorphic clasts in upper Toarcian strata (Dickie & Hein, 1995; Hart et al., 1995; Johannson et al., 1997; Shirmohammad et al., 2011). Eclogite clasts occur locally in Pliensbachian-Toarcian strata of the Laberge Group in northern British Columbia (Figure 11; Canil et al., 2006). They record rapid exhumation in the Early Jurassic (Kellett et al., 2018). Chert clasts are locally present in Bajocian strata in Yukon (Colpron et al., 2015) and are abundant in strata of this age in northern British Columbia (Shirmohammad et al., 2011).

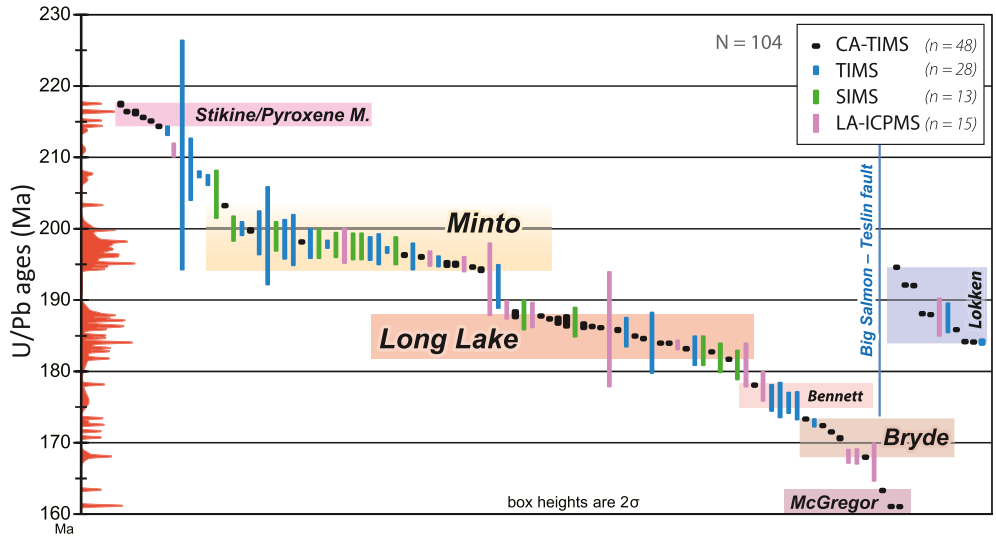

Figure 12. Ranked plot of U/Pb zircon ages for all Late Triassic to Jurassic igneous samples analyzed from the Intermontane terranes in Yukon (data from Yukon Geological Survey, 2020c). Data points are shown with 2σ errors and color-coded according to analytical technique. Data for the Lokken suite, east of the BSTF, are shown separately at right. A probability density plot for ages from plutons west of the BSTF is shown in red at left (n = 92). The age ranges of plutonic suites determined from CA-TIMS dates (Figure 4) are indicated by color boxes.

Detrital zircon provenance studies show that Laberge Group rocks were locally derived from basement sources on the flanks of WT (Colpron et al., 2015; van Drecht, 2019). Late Triassic-Early Jurassic zircons make the dominant age peaks in Laberge sandstones with Paleozoic (mainly Carboniferous) zircons representing subordinate but locally significant populations. This pattern matches igneous ages from plutons surrounding the WT (Colpron et al., 2015) and inherited zircons in Jurassic plutons (Figures 3, 4, and 9). The Hf isotopic signatures of detrital zircons in sandstones of the Laberge Group show a shift from superchondritic to subchondritic values between Late Triassic and Early Jurassic (van Drecht, 2019), a pattern that mimics the trend observed in Late Triassic and Jurassic plutons in Yukon (Figure 6c).

Final imbrication of the Intermontane terranes in Middle Jurassic (Aalenian-Bajocian) brought the end of marine deposition in the WT, local tilting of Laberge strata, surface uplift, and deposition of the overlying Upper Jurassic to Lower Cretaceous Tantalus Formation in fluvial and lacustrine settings within confined intermontane valleys (Long, 2015). Detrital zircons in the Tantalus Formation have mainly similar sources as, or were recycled from Laberge Group strata, with exception of minor Late Jurassic populations that Colpron et al. (2015) attributed to ash-fall from distal volcanic sources in the Insular terranes. New CA-TIMS dates from the main phase of the McGregor batholith (163–161 Ma; Figure 4) and a $^{40}Ar/^{39}Ar$ muscovite age of ca. 146 Ma from its younger phase (Sack et al., 2020) indicate that local sources are available for Late Jurassic zircons in the Tantalus Formation.

5. Discussion

5.1. Improved Geochronology and Tempos of Magmatism

The new zircon CA-TIMS U-Pb dates produced for this study provide tight constraints on the duration of pluton emplacement in southern Yukon (Figure 4). These data indicate that Late Triassic to Early Jurassic suites that intrude Stikinia and Yukon-Tanana terrane west of the BSTF were emplaced in discrete episodes of 2–5 Myr in duration, possibly as long as 8–9 Myr for the Minto suite. These new data bring refinement over the apparent continuum in magmatism from Late Triassic to Middle Jurassic suggested when all U-Pb zircon dates acquired from these plutons are considered, including ages determined using less precise analytical techniques such as LA-ICPMS, secondary ion mass spectrometry (SIMS), and TIMS on multi-grain, air-abraded zircon fractions (Figure 12). The large batholiths of the Minto suite were primarily constructed over ~3.5 Myr between 198.22 and 194.71 Ma (Figures 4 and 12). Older, ca. 205–203 Ma phases are locally documented and the common occurrence of ca. 205–203 Ma zircon ante-

crysts suggest that Minto magmatism may have lasted up to 8–9 Myr. Construction of the Aishihik batholith (Long Lake suite; Figure 3) occurred over ~3 Myr between 186.22 and 183.28 Ma, and the full range of Long Lake magmatism lasted ~4.6 Myr, from 187.46 to 182.83 Ma (Figures 4 and 12). The Lokken suite, east of the BSTF, spans 9 Myr and includes a magmatic pulse at ca. 192 Ma during an apparent lull between the Minto and Long Lake suites to the west (Figures 4 and 12). The tempos of magmatism indicated from the range of CA-TIMS dates in Early Jurassic plutons in Yukon are consistent with construction rates of ≤10 Myr determined for other well-studied large batholiths (e.g., Coleman et al., 2004; Frazer et al., 2014; Glazner et al., 2004; Schwartz et al., 2017).

Limited CA-TIMS data for the Bennett suite precludes exact estimate of the intrusive rate for these plutons, however when considering previous TIMS dates a tempo of ~3 Myr is also indicated. Plutons of the Middle Jurassic Bryde suite were mostly intruded in <2 Myr, between 173.44 and 172.62 Ma (Figures 4 and 12). The 168.09 Ma Michie pluton could represent continuum of Bryde suite magmatism over ~5.4 Myr or a distinct, younger pulse of magmatism. In northern British Columbia, Mihalynuk et al. (2004, 2018) estimated a range of ca. 172–166 Ma for the Fourth of July suite based on U-Pb zircon TIMS, and K-Ar and $^{40}Ar/^{39}Ar$ biotite dates.

5.2. Sources of Inheritance

Inherited zircon cores were documented in 15 of 30 Jurassic samples analyzed both by LA-ICPMS and CA-TIMS (Figures 3 and 9). A total of 129 cores were analyzed with 54% yielding Triassic to Jurassic (ca. 235–187 Ma), 37% Devonian to Carboniferous (ca. 378–306 Ma), 4% Permian (ca. 275–250 Ma), and 5% Precambrian dates (ca. 2,606–571 Ma; Figure 9e). Late Triassic cores (peak at 213 Ma) are most common in the Minto suite, although Paleozoic cores make up the majority of zircon xenocrysts analyzed in these samples (68%; Figure 9a). The Late Triassic zircon cores have juvenile εHf_t values (+3.2 to +6.0), similar to those of the Stikine-Lewes River arc (whole rock εHf_t +3.2 to +10.6; Figure 9f); this is consistent with the local abundance of variably migmatized xenoliths of Late Triassic intermediate to mafic rocks in plutons of the Minto suite (Kovacs et al., 2020; Sack et al., 2020).

Inherited zircons in samples of the Long Lake, Lokken, and McGregor suites are dominated by latest Triassic to Early Jurassic dates (ca. 209–193 Ma) with ca. 199 Ma peaks and εHf_t values of −6.0 to +9.3 (Figure 9). These peaks match well with the age range of the Minto suite (Figure 4), but igneous zircons from these plutons are consistently superchondritic (εHf_t +0.5 to +10.9; Figure 6). Occurrences of Minto-age xenocrysts in Early Jurassic granitoids from both sides of the BSTF point to similarity in latest Triassic to earliest Jurassic magmatic activity, although plutons older than ca. 195 Ma are not documented in the Lokken suite in Yukon. The oldest phases in the Hogem batholith of central British Columbia (Figure 1) are ca. 207–194 Ma (Jones et al., 2021) and older plutons (ca. 215–205 Ma) are common in southern Quesnellia (Han et al., 2020; Mortensen et al., 1995).

Inherited zircons with Paleozoic dates are present in all suites and generally match well the ages and Hf isotopic composition of local Paleozoic units in Yukon-Tanana and Stikinia (Figure 9f). The Late Devonian inherited zircons (ca. 378–374 Ma) with mostly subchondritic εHf_t values in the Aishihik batholith (Long Lake suite) are the exception (Figure 9). There are no known sources in local rocks of Stikinia or Yukon-Tanana terrane for these zircons. In southern Yukon, ca. 378–373 Ma volcanism is only documented in continental margin strata of the Earn Group, presently ~250 km away northeast of the Tintina fault (Cobbett et al., 2021; Yukon Geological Survey, 2020a, 2020b, 2020c). Zircons within this age range are also documented in the Yukon-Tanana terrane of southeast Alaska (>400 km south) but consistently have superchondritic εHf_t values (Pecha et al., 2016). Rare Precambrian zircons in Early Jurassic plutons in Yukon were likely recycled through incorporation of minor metasedimentary sources in the Yukon-Tanana terrane (e.g., Snowcap assemblage; Piercey & Colpron, 2009).

5.3. Spatial Versus Temporal Isotopic Patterns

Armstrong (1988) showed that the regional distribution of $^{87}Sr/^{86}Sr_i$ isopleths in Mesozoic igneous rocks of the Canadian Cordillera defines a hairpin geometry with juvenile values (≤0.704) in the core of the Intermontane terranes surrounded by more evolved values (≥0.705) in central Yukon. This pattern was one of the lines of evidence that led to the oroclinal entrapment model of Mihalynuk et al. (1994). The new isotopic data reported here confirm the general patterns of $^{87}Sr/^{86}Sr_i$ isopleths (Figure 7a) observed by Armstrong (1988) but with the added benefit of improved geochronological constraints (Figure 4). As noted above, the isotopic evolution of Late Triassic and Jurassic plutons in southern Yukon is directly linked with the age of magmatism, with Early

Jurassic plutons west of the BSTF yielding more evolved values in progressively younger plutons, and those east of the BSTF showing a reverse trend (Figure 6). Juvenile isotopic values are mainly documented in plutons of the Late Triassic Stikine suite and Middle Jurassic Bryde suite that only occur southwest of the BSTF (Figure 7). Juvenile $^{87}Sr/^{86}Sr_i$ (<0.704) values are only documented in one pluton of the Lokken suite, east of the BSTF, and the distribution of isopleths is likely somewhat modified by Cretaceous or younger displacement along the fault zone.

5.4. Redefining Terrane Boundaries

The difference in style of Early Jurassic magmatism across the BSTF provides new constraints on locating the boundary between Stikinia and Quesnellia in central Yukon (Figures 3 and 11). In British Columbia, the two arc terranes occur on either side of the Cache Creek accretionary complex, but in Yukon the absence of Cache Creek rocks north of ~61°N have made the distinction between Stikinia and Quesnellia difficult (Figure 1). The Thibert fault marks the boundary between Quesnellia and Cache Creek terranes in northern British Columbia and its extension in Yukon, the Teslin fault, has traditionally been inferred to mark the Quesnellia-Stikinia boundary (Colpron, 2011; Colpron, Israel, Murphy, et al., 2016; Gordey & Makepeace, 2001; White et al., 2012). Near 62°N in central Yukon, seismic and gravity results suggest that the Big Salmon fault is a more significant crustal structure than the Teslin fault (Calvert et al., 2017).

The peraluminous plutons of the Minto suite that were emplaced at lower crustal levels are restricted to the west of the BSTF (Figures 2 and 3). East of Carmacks, the Tatchun batholith intrudes Carboniferous rocks of the Boswell assemblage and overlying Upper Triassic volcanic rocks of the Semenof formation (Colpron, 2011; Tempelman-Kluit, 1984, 2009). Augite-phyric volcanic and volcaniclastic rocks and minor Carnian-Norian limestone of the Semenof formation resemble coeval strata of the Lewes River Group to the west (Figure 2). They unconformably overlie mafic to intermediate metavolcanic, metavolcaniclastic, and metasedimentary rocks (Boswell assemblage) which have been interpreted to represent local Paleozoic basement to Quesnellia (Colpron, 2011). Their association with Minto suite plutons suggests, however, that they are part of the same crustal panel as Stikinia west of the Teslin fault.

East of the BSTF, metaluminous plutons of the Lokken suite were emplaced at higher crustal levels into part of the Yukon-Tanana terrane that includes strata of the Klinkit assemblage, which are correlated with Paleozoic arc successions of Quesnellia in British Columbia (Lay Range assemblage; Ferri, 1997; Nelson & Friedman, 2004; Nixon et al., 2020; Roots et al., 2006; Simard et al., 2003). The Lokken suite is generally more mafic than Early Jurassic plutons west of the BSTF and locally includes ultramafic phases (Roots et al., 2004). Upper Triassic rocks overlying Yukon-Tanana east of the BSTF are fine-grained siliciclastic rocks and local conglomerate that are inferred to correlate with those overlapping the western Laurentian margin (Beranek & Mortensen, 2011; Colpron, Nelson, & Murphy, 2006; Colpron, Mortensen, et al., 2006; Golding et al., 2016; Unterschutz et al., 2002).

The present crustal architecture of the Intermontane terranes in central Yukon was acquired through superposition of Jurassic to Late Cretaceous (and younger) structures (Calvert et al., 2017; Nelson et al., 2013). The Cretaceous structures dissected and overprinted older Jurassic faults such as the Tadru and Needlerock faults (Figures 2 and 3; Colpron et al., 2002, 2003). The Needlerock thrust is a folded thrust fault that juxtaposes the Snowcap assemblage (Yukon-Tanana terrane) in its hanging wall with greenstone and amphibolite of the Boswell assemblage in its footwall. The Boswell assemblage was intruded at mid to lower crustal level by the Tatchun batholith (Minto suite) in the Early Jurassic, suggesting that the Needlerock thrust may be a remnant of the Jurassic boundary between Stikinia to the west and Yukon-Tanana/Quesnellia to the east. Extension of the Needlerock thrust, and the Stikinia-Quesnellia boundary, into western Yukon remains enigmatic.

5.5. Relationship to Hazelton Arc

The syn-collisional intrusion of Early Jurassic plutons and development of the WT north of the Stikine arch contrasts with continued Early to Middle Jurassic arc activity recorded in volcano-sedimentary strata of the Hazelton Group to the south (Figure 11; Gagnon et al., 2012; George et al., 2021; Nelson et al., 2018, 2022). Widespread exposures of the Hazelton Group across 300 km in northern British Columbia, between the Stikine and Skeena arches, were interpreted by Marsden and Thorkelson (1992) to result from development of two magmatic arcs above opposing subduction zones on either side of Stikinia. However, more recent studies show that Rhaetian to Toarcian arc magmatism in the lower Hazelton Group focused on an arcuate belt that spans the Skeena arch

(including the Telkwa and Toodoggone formations) and that coeval magmatism in the Stewart-Iskut region formed in the back-arc (Figure 11; George et al., 2021; Nelson et al., 2018, 2022). The onset of lower Hazelton arc magmatism (ca. 205-200 Ma) coincides with initial collision and intrusion of the Minto suite north of the Stikine arch. Following initial collision, the Hazelton arc is inferred to have migrated southward through the Early Jurassic. Subduction rollback was accommodated by north-south extension and subsidence in the back-arc region (e.g., Diakow et al., 1993; Diakow & Rhodes, 2006; Gagnon et al., 2009; Nelson et al., 2022). Sinistral transpression along structures such as the Llewellyn and Wann River faults (Currie & Parrish, 1993; Mihalynuk et al., 1999) probably linked the retreating Hazelton arc with the collision zone, Early Jurassic extensional exhumation of the Yukon-Tanana terrane, and subsidence of the WT north of the Stikine arch (Figure 11). Early Jurassic syn-collisional plutons in Stikinia north of the Stikine arch show a southward migration that suggests that the source of magmatism remained tied to the supra-subduction mantle wedge associated with the retreating Hazelton arc.

South of the Stikine arch, post-arc extension and subsidence is recorded by predominantly sedimentary strata of the upper Hazelton Group (Pliensbachian-Callovian), which onlapped the arch in Toarcian, and development of the Eskay rift in Aalenian-Bajocian (Barresi et al., 2015; Gagnon et al., 2012; Nelson et al., 2018). The Hazelton Group is conformably overlain by southward-propagating synorogenic clastic rocks of the Middle Jurassic to Lower Cretaceous Bowser Lake Group (Evenchick et al., 2007, 2010).

Detrital zircons in sandstones from the Hazelton Group are dominated by Triassic and Jurassic ages that resemble age distribution in strata of the Laberge Group in Yukon (Colpron et al., 2015; George et al., 2021). However, Triassic-Jurassic zircons in the Hazelton Group in central Stikinia have consistently juvenile εHf_t values (George et al., 2021) that contrast with the isotopic pull-down observed in detrital zircons from the Laberge Group (van Drecht, 2019) and in igneous zircons from Early Jurassic syn-collisional plutons of southern Yukon (Figure 6c).

5.6. Tectonic Evolution

Over the last 25 yr, the oroclinal entrapment of the Cache Creek terrane has been the prevalent tectonic model for the Jurassic evolution of the Intermontane terranes in the Canadian Cordillera (Colpron et al., 2015; Mihalynuk et al., 1994, 2004; Nelson et al., 2013; Nelson & Mihalynuk, 1993). In this model, similar late Paleozoic-early Mesozoic arc terranes of Stikinia and Quesnellia, which include Permian and Triassic fauna endemic to southern Laurentia (Belasky et al., 2002; Stanley & Senowbari-Daryan, 1999; Stevens, 1995), were oroclinally folded around the accretionary complex of the Cache Creek terrane containing Permian faunal elements of Tethyan (exotic) affinity (Ross & Monger, 1978; Ross & Ross, 1983). Oroclinal enclosure was thought to be triggered by introduction of oceanic plateaus (Mihalynuk et al., 1994) or primitive arc crust (Kutcho assemblage; Colpron et al., 2015) into the Late Triassic subduction zone, and the axial region of the Stuhini-Lewes River arc rotated counterclockwise around a hinge zone in the Yukon-Tanana terrane relative to the arc axis of Quesnellia. A challenge with this model is the implied $\geq 90°$ rotation, around a vertical axis, of a subduction zone with slab width $\geq$2,000 km that would have been characterized by a southward increase in retreat velocities of the trench, possibly exceeding 12 cm/yr near the south end of Stikinia (assuming angular rotation of as much as 2,500 km in ~20 Myr). Modeling of modern subduction zones, however, shows that for slabs $\geq$2,000 km trench retreat velocities are slow (to nearly stationary) near the center of the slab, generally $\leq$2 cm/yr (Schellart et al., 2007). Faster velocities (up to 6–16 cm/yr) are only observed in narrow slabs ($\leq$1,500 km) with curved, convex geometries, such as the Oligocene to Holocene Scotia and Calabrian subduction zones. Additionally, three-dimensional numerical modeling of continental ribbons with horizontally stratified lithosphere (as observed in arc crust; Calvert, 2011) show that horizontal-axis folding and thickening of the lithosphere is more probable than vertical-axis rotation of an orocline (Smith et al., 2021). Thus, it is improbable that the Stikinia subduction zone was subject of wholesale angular rotation in the Early Jurassic, as implied in some recent models (Colpron et al., 2015; Logan & Mihalynuk, 2014). Alternative models invoking strike-slip duplication of the Quesnellia-Stikinia arc have been proposed (Wernicke & Klepacki, 1988), but fail to explain the concentric south-facing patterns of geological elements in the northern Intermontane terranes (Figures 1 and 2). Detailed documentation of the Early Jurassic collision zone north of the Stikine arch provides new constraints and the basis for an alternative model (Figure 13).

The configuration of Triassic arc terranes outboard of western Laurentia is inferred to have resembled a mirror image of the present-day geometry of the western Aleutian and Kamchatka subduction zones, where parts of Quesnellia (and its Yukon-Tanana basement in the north) were anchored on the margin of western Pangea

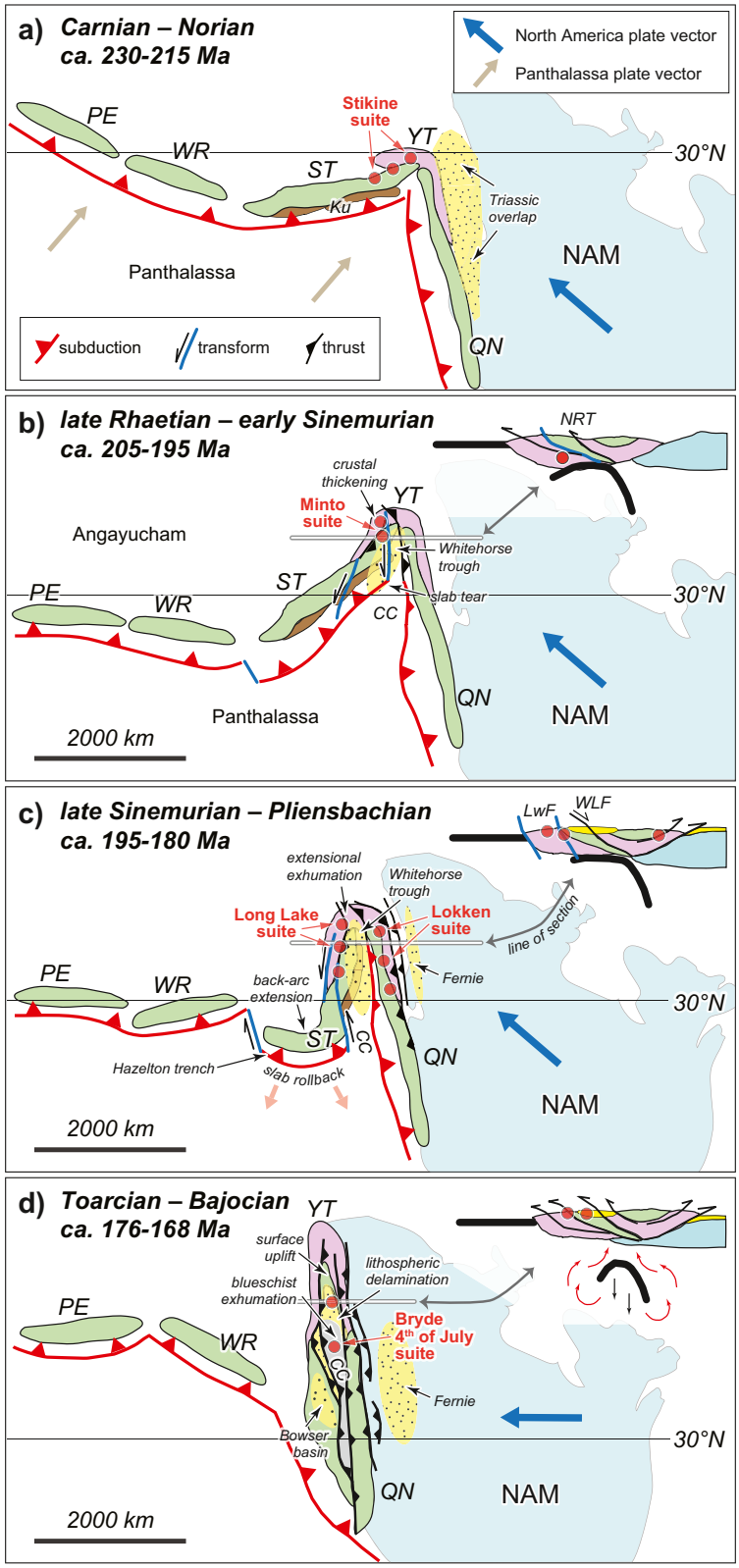
a) Carnian – Norian
ca. 230-215 Ma
North America plate vector
Panthalassa plate vector
PE
WR
Stikine suite
YT
ST
Ku
30°N
Triassic overlap
NAM
Panthalassa
subduction
transform
thrust
QN
b) late Rhaetian – early Sinemurian
ca. 205-195 Ma
NRT
crustal thickening
Minto suite
YT
Angayucham
Whitehorse trough
PE
WR
ST
slab tear
CC
30°N
QN
NAM
Panthalassa
2000 km
c) late Sinemurian – Pliensbachian
ca. 195-180 Ma
LwF
WLF
extensional exhumation
Whitehorse trough
Long Lake suite
Lokken suite
line of section
PE
WR
back-arc extension
Fernie
30°N
ST
CC
QN
Hazelton trench
slab rollback
NAM
2000 km
d) Toarcian – Bajocian
ca. 176-168 Ma
YT
surface uplift
lithospheric delamination
blueschist exhumation
PE
WR
Bryde 4th of July suite
CC
Fernie
30°N
Bowser basin
QN
NAM
2000 km

Figure 13.

(Beranek & Mortensen, 2011; Unterschutz et al., 2002) and Stikinia extended westward into an intra-oceanic island arc festoon (Figure 13a; Colpron et al., 2015; George et al., 2021; Mihalynuk et al., 1994). Plutons of the Stikine and Pyroxene Mountain suites in Yukon indicate that Stikinia was locally anchored on the Yukon-Tanana terrane by the Late Triassic. Other parts of the Late Triassic Stikinia arc (present-day northern and central British Columbia) appear to have been constructed on distinct Paleozoic basement with probable affinity to the Insular terranes (George et al., 2021). Late Triassic (Carnian-Norian) volcanic and sedimentary rocks of Stikinia also unconformably overlie Middle Triassic volcanic units that form part of the Kutcho assemblage in southern Yukon and northern British Columbia and indicate juxtaposition prior to development of the Stikine arc (e.g., Bordet et al., 2019; Logan et al., 2012; Schiarizza, 2012). This postulated arc configuration suggests that plate motion in Panthalassa was northeasterly in the Late Triassic.

End-on arc collision in northern Stikinia was likely triggered by onset of the northwestward drift of North America as break-up of the Pangea supercontinent began in latest Triassic (Coney, 1972; Dickinson, 2004; Monger & Gibson, 2019). This resulted in initial imbrication and crustal thickening of the northern Intermontane terranes, north of the Stikine arch, and intrusion of Minto suite plutons that are transitional between arc and syn-collisional granitoids and show increased crustal influence (Figures 6 and 13b). Subduction waned beneath the Stuhini-Lewes River arc north of the Stikine arch and part of the slab was reconfigured into a shorter segment above which the Hazelton arc was developed to the south (Nelson et al., 2022). The Sinemurian exhumation of eclogite bodies, recorded as clasts in Pliensbachian strata of the Laberge Group (Kellett et al., 2018), may have been facilitated by slab tear associated with this subduction reconfiguration. To the east, subduction of Panthalassa lithosphere continued beneath Quesnellia (Figure 13b).

Between Sinemurian and Toarcian, the Hazelton trench retreated to the south and back-arc extension occurred south of the Stikine arch (Figure 13c; Nelson et al., 2022). This evolving arc–back-arc system was probably linked to the collision zone to the north by sinistral strike-slip faults such as the Llewelyn fault (Figure 11). Sinistral transtension likely accommodated extensional exhumation of the burgeoning orogen and subsidence of the WT to the north (van Drecht, 2019). Subsidence may have been aided by underplating of mafic crust and development of an eclogitic root after cessation of Late Triassic subduction. Isotopically evolved granitoid plutons of the Long Lake and Bennett suites were emplaced within the exhuming orogen. In this revised model, entrapment of the Cache Creek terrane occurred as a result of development of sinistral transform faults that were linked to the retreating Hazelton subduction zone.

Continued westward drift of North America, as opening of the central Atlantic Ocean began, possibly as early as late Sinemurian (Labails et al., 2010), resulted in convergence of the Intermontane terranes with the North American continental margin in late Sinemurian to Pliensbachian (Murphy et al., 1995; Nixon et al., 1997, 2020). Paleomagnetic data and faunal assemblages from strata in Stikinia suggest it was ~$11.2° \pm 6.1°$ ($1{,}200 \pm 680$ km) south of its present position relative to the North American craton in late Sinemurian to early Pliensbachian (Kent & Irving, 2010; Smith, 2006; Smith et al., 2001). The collision zone now located in southern Yukon was then probably at similar latitude as present-day southern Aberta, and the easterward convergence of the accreted terranes likely drove the onset of subsidence and deposition of the Fernie Formation in the Alberta foreland basin (Figure 13c; Asgar-Deen, 2003; Cant & Stockmal, 1989; Colpron et al., 2015; McCartney, 2012; Pană et al., 2018).

By Middle Jurassic, subduction had ceased beneath Quesnellia, blueschists were exhumed in the northern Cache Creek terrane, and the Intermontane terranes were imbricated along a series of west-verging thrust faults (Figure 13d; Mihalynuk et al., 2004). The post-collisional plutons of the Bryde suite are characterized by a return to isotopically juvenile magmatism at ca. 174 Ma (Figure 6) that suggests asthenospheric upwelling following terrane imbrication. This coincides with surface uplift that marked the end of marine deposition in WT and development of intermontane river systems recorded in strata of the Tantalus Formation. The combination of juvenile magmatism and surface uplift suggests that lithospheric delamination or slab breakoff occurred following final

Figure 13. Schematic representation of paleogeography and tectonic evolution of the Intermontane terranes and northwestern edge of North America in Late Triassic to Middle Jurassic (a)–(d). Schematic section across southern Yukon shown in upper right in (b)–(d). Relative position of plutonic suites discussed in this paper are shown by red dots. Synorogenic clastic rocks are shown by yellow stippled pattern. Terrane labels: *Abbrrviations*. CC, Cache Creek; Ku, Kutcho (including Sitlika-Wineglass-Venables assemblages; Logan & Mihalynuk, 2014); PE, Peninsular; QN, Quesnellia; ST, Stikinia; WR, Wrangellia; YT, Yukon-Tanana. Fault labels in cross-sections: *Abbreviations*. LwF, Lewellyn fault; NRT, Needlerock thrust; WLF, Willow Lake fault.

collision of the northern Intermontane terranes (e.g., Davies & von Blanckenburg, 1995; Kay & Kay, 1993; von Blanckenburg & Davies, 1995).

6. Conclusions

The Late Triassic to Jurassic plutons in the Intermontane terranes of Yukon record the transition from arc to syn- and post-collisional magmatism. Juvenile Late Triassic magmatism of the Stikine and Pyroxene Mountain suites represent the northern extension of the Stikinia arc that locally intrudes the Yukon-Tanana terrane in Yukon and Alaska. The Early Jurassic plutons west of the BSTF in Yukon were intruded into a thickening orogen and show increasing crustal contributions with time. This contrasts with coeval, juvenile magmatism of the Hazelton arc in British Columbia that apparently records a southward arc migration in the Early Jurassic. East of the BSTF, Early Jurassic plutons that intrude into Yukon-Tanana basement are the northern extension of Quesnellia arc magmatism. Syn-collisional, Early Jurassic magmatism in Yukon is interpreted to result from end-on arc collision in northern Stikinia. Exhumation of the Yukon-Tanana terrane and coeval subsidence in the WT developed as a result of sinistral transtension linked to the retreating Hazelton trench to the south. A revised tectonic model shows that entrapment of the Cache Creek terrane is the result of Hazelton slab rollback and development of sinistral transform faults that originated from the collision zone to the north. The continued westward drift of the North American continent resulted in imbrication and final accretion of the Intermontane terranes in the Middle Jurassic. This was accompanied by lithospheric delamination as indicated by a return to juvenile magmatism in Middle Jurassic and surface uplift that marked the end of marine deposition in the WT.

Data Availability Statement

Data for this article are available for download from the following references: Sack et al. (2020), http://data.geology.gov.yk.ca/Reference/95839 and Sack et al. (2022), https://data.geology.gov.yk.ca/Reference/95925.

Acknowledgments
Discussions with JoAnne Nelson, Sarah George, and Bram van Straaten provided insights in developing the alternative model proposed in this article. Comments by Bill McClelland, Jim Monger, Don Murphy, and JoAnne Nelson on early versions of the manuscript has helped to sharpen the arguments. Formal reviews by Mitch Mihalynuk and an anonymous reviewer, and editorial advices by Associate Editor Robinson Cecil are gratefully acknowledged. This study was funded by the Yukon Geological Survey with additional support by Natural Resources Canada's Geomapping for Energy and Minerals program. This work is Yukon Geological Survey contribution #058.

References

Anderson, J. L., & Smith, D. R. (1995). The effects of temperature and fO_2 on the Al-in-hornblende barometer. *American Mineralogist*, *80*, 549–559. https://doi.org/10.2138/am-1995-5-614

Armstrong, R. L. (1988). Mesozoic and early Cenozoic magmatic evolution of the Canadian Cordillera. In S. P. Clark Jr, B. C. Burchfield, & J. Suppe (Eds.), *Processes in continental lithospheric deformation, special paper* (Vol. 218, pp. 55–92). Geological Society of America. https://doi.org/10.1130/spe218-p55

Asgar-Deen, M. (2003). *Stratigraphy, sedimentology and paleogeography of the Lower Jurassic Nordegg Member (Gordondale Member), west-central Alberta* (master's thesis). University of Calgary.

Barresi, T., Nelson, J. L., Dostal, J., & Friedman, R. M. (2015). Evolution of the Hazelton arc near Terrace, British Columbia: Stratigraphic, geochronological, and geochemical constraints on a Late Triassic-Early Jurassic arc and Cu-Au porphyry belt. *Canadian Journal of Earth Sciences*, *52*, 466–494. https://doi.org/10.1139/cjes-2014-0155

Beatty, T. W., Orchard, M. J., & Mustard, P. S. (2006). Geology and tectonic history of the Quesnel terrane in the area of Kamloops, British Columbia. In M. Colpron, & J. L. Nelson (Eds.), *Paleozoic evolution and metallogeny of Pericratonic terranes at the Ancient Pacific Margin of North America, special paper* (Vol. 45, pp. 483–504). Geological Association of Canada.

Belasky, P., Stevens, C. H., & Hanger, R. A. (2002). Early Permian location of western North American terranes based on brachiopod, fusulinid and coral biogeography. *Palaeogeography, Palaeoclimatology, Palaeoecology*, *179*, 245–266. https://doi.org/10.1016/s0031-0182(01)00437-0

Beranek, L. P., & Mortensen, J. K. (2011). The timing and provenance record of the Late Permian Klondike orogeny in northwestern Canada and arc-continent collision along western North America. *Tectonics*, *30*, TC5017. https://doi.org/10.1029/2010tc002849

Berman, R. G., Ryan, J. J., Gordey, S. P., & Villeneuve, M. (2007). Permian to Cretaceous polymetamorphic evolution of the Stewart River region, Yukon-Tanana terrane, Yukon, Canada: P–T evolution linked with in situ SHRIMP monazite geochronology. *Journal of Metamorphic Geology*, *25*, 803–827. https://doi.org/10.1111/j.1525-1314.2007.00729.x

Bickerton, L., Colpron, M., Gibson, H. D., Thorkelson, D. J., & Crowley, J. L. (2020). The northern termination of the Cache Creek terrane in Yukon: Middle Triassic arc activity and Jurassic-Cretaceous structural imbrication. *Canadian Journal of Earth Sciences*, *57*, 227–248. https://doi.org/10.1139/cjes-2018-0262

Bordet, E., Crowley, J. L., & Piercey, S. J. (2019). *Geology of eastern Lake Laberge area (105E), south-central Yukon* (open file 2019-1). Yukon Geological Survey.

British Columbia Geological Survey. (2019). *BC MINFILE – A database of mineral occurrences*. Retrieved from https://www2.gov.bc.ca/gov/content/industry/mineral-exploration-mining/british-columbia-geological-survey/mineralinventory

Brown, D., Ryan, P. D., Afonso, J. C., Boutelier, D., Burg, J.-P., Byrne, T., et al. (2011). Arc–continent collision: The making of an orogen. In D. Brown, & P. D. Ryan (Eds.), *Arc–continent collision. Frontiers in earth sciences* (pp. 477–493). Springer-Verlag. https://doi.org/10.1007/978-3-540-88558-0_17

Brown, D. A., Gunning, M. H., & Greig, C. J. (1996). *The Stikine project: Geology of western Telegraph Creek map area, northwestern British Columbia (NTS 104G/5, 6, 11W, 12 and 13). (Bulletin 95)*. British Columbia Geological Survey.

Calvert, A. J. (2011). The seismic structure of island arc crust. In D. Brown, & P. D. Ryan (Eds.), *Arc-continent collision. Frontiers in earth sciences* (pp. 87–119). Springer-Verlag. https://doi.org/10.1007/978-3-540-88558-0_4

Calvert, A. J., Hayward, N., Vayavur, R., & Colpron, M. (2017). Seismic and gravity constraints on the crustal architecture of the Intermontane terranes, central Yukon. *Canadian Journal of Earth Sciences*, *54*, 798–811. https://doi.org/10.1139/cjes-2016-0189

Canil, D., Mihalynuk, M. G., & Charnell, C. (2006). Sedimentary record for exhumation of ultrahigh pressure (UHP) rocks in the northern Cordillera, British Columbia, Canada. *Geological Society of America Bulletin*, *118*, 1171–1184. https://doi.org/10.1130/b25921.1

Cant, D. J., & Stockmal, G. S. (1989). The Alberta foreland basin: Relationship between stratigraphy and Cordilleran terrane-accretion events. *Canadian Journal of Earth Sciences*, *26*, 1964–1975. https://doi.org/10.1139/e89-166

Cawood, P. A., Kröner, A., Collins, W. J., Kusky, T. M., Mooney, W. D., Windley, B. F., & Geological Society of London. (2009). Accretionary orogens through Earth history. In P. A. Cawood, & A. Kröner (Eds.), *Earth accretionary systems in space and time* (Vol. 318, pp. 1–36). Geological Society, London, Special Publications. https://doi.org/10.1144/sp318.1

Clark, A. D. (2017). *Tectonometamorphic history of mid-crustal rocks at Aishihik Lake, southwest Yukon* (master's thesis). Simon Fraser University.

Cobbett, R., Colpron, M., Crowley, J. L., Cordey, F., Blodgett, R. B., & Orchard, M. J. (2021). Late Devonian magmatism and clastic deposition in the upper Earn Group (central Yukon) mark the transition from passive to active margin along western Laurentia. *Canadian Journal of Earth Sciences*, *58*, 471–494. https://doi.org/10.1139/cjes-2020-0161

Coleman, D. S., Gray, W., & Glazner, A. F. (2004). Rethinking the emplacement and evolution of zoned plutons: Geochronologic evidence for incremental assembly of the Tuolumne Intrusive Suite, California. *Geology*, *32*, 433–436. https://doi.org/10.1130/g20220.1

Colpron, M. (2011). *Geological compilation of Whitehorse trough – Whitehorse (105D), Lake Laberge (105E), and part of Carmacks (115I), Glenlyon (105L), Aishihik Lake (115H), Quiet Lake (105F) and Teslin (105C) (Geoscience map 2011-1)*. Yukon Geological Survey.

Colpron, M., Crowley, J. L., Gehrels, G. E., Long, D. G. F., Murphy, D. C., Beranek, L. P., & Bickerton, L. (2015). Birth of the northern Cordilleran orogen, as recorded by detrital zircons in Jurassic synorogenic strata and regional exhumation in Yukon. *Lithosphere*, *7*, 541–562. https://doi.org/10.1130/l451.1

Colpron, M., & Friedman, R. M. (2008). U-Pb zircon ages for the Nordenskiold formation (Laberge Group) and Cretaceous intrusive rocks, Whitehorse trough, Yukon. In D. S. Emond, L. R. Blackburn, R. P. Hill, & L. H. Weston (Eds.), *Yukon exploration and geology 2007* (pp. 139–151). Yukon Geological Survey.

Colpron, M., Israel, S., & Friend, M. (2016). *Yukon plutonic suites* (open file 2016-37). Yukon Geological Survey.

Colpron, M., Israel, S., Murphy, D. C., Pigage, L. C., & Moynihan, D. (2016). *Yukon bedrock geology map* (open file 2016-1). Yukon Geological Survey.

Colpron, M., Mortensen, J. K., Gehrels, G. E., & Villeneuve, M. E. (2006). Basement complex, Carboniferous magmatism and Paleozoic deformation in Yukon-Tanana terrane of central Yukon: Field, geochemical and geochronological constraints from Glenlyon map area. In M. Colpron, & J. L. Nelson (Eds.), *Paleozoic evolution and metallogeny of pericratonic terranes at the Ancient Pacific Margin of North America, Canadian and Alaskan Cordillera special paper* (Vol. 45, pp. 131–151). Geological Association of Canada.

Colpron, M., Murphy, D. C., Nelson, J. L., Roots, C. F., Gladwin, K., Gordey, S. P., & Abbott, J. G. (2003). Yukon targeted geoscience initiative, Part 1: Results of accelerated bedrock mapping in Glenlyon (105L/1-7,11-14) and northeast Carmacks (115I/9,16) areas, central Yukon. In D. S. Emond, & L. L. Lewis (Eds.), *Yukon exploration and geology 2002* (pp. 85–108). Yukon Geological Survey.

Colpron, M., Murphy, D. C., Nelson, J. L., Roots, C. F., Gladwin, K., Gordey, S. P., et al. (2002). *Preliminary geological map of Glenlyon (105L/1-7,11-14) and northeast Carmacks (115I/9,16) areas, Yukon Territory (1:125 000 scale)* (open file 2002-9). Yukon Geological Survey.

Colpron, M., & Nelson, J. L. (2011). *A digital atlas of terranes for the northern Cordillera*. Yukon Geological Survey. Retrieved from http://data.geology.gov.yk.ca/Compilation/2

Colpron, M., Nelson, J. L., & Geological Society of London. (2009). A Palaeozoic Northwest Passage: Incursion of Caledonian, Baltican and Siberian terranes into eastern Panthalassa, and the early evolution of the north American Cordillera. In P. A. Cawood, & A. Kröner (Eds.), *Earth accretionary systems in space and time* (Vol. 318, pp. 273–307). Geological Society, London, Special Publications. https://doi.org/10.1144/sp318.10

Colpron, M., Nelson, J. L., & Murphy, D. C. (2006). A tectonostratigraphic framework for the pericratonic terranes of the northern Cordillera. In M. Colpron, & J. L. Nelson (Eds.), *Paleozoic evolution and metallogeny of pericratonic terranes at the Ancient Pacific Margin of North America, Canadian and Alaskan Cordillera special paper* (Vol. 45, pp. 1–23). Geological Association of Canada.

Colpron, M., Nelson, J. L., & Murphy, D. C. (2007). Northern Cordilleran terranes and their interactions through time. *Geological Society of America Today*, *17*(4/5), 4–10. https://doi.org/10.1130/gsat01704-5a.1

Colpron, M., & Ryan, J. J. (2010). Bedrock geology of southwest McQuesten (NTS 115P) and part of northern Carmacks (NTS 115I) map area. In K. E. MacFarlane, L. H. Weston, & L. R. Blackburn (Eds.), *Yukon exploration and geology 2009* (pp. 159–184). Yukon Geological Survey.

Coney, P. J. (1972). Cordilleran tectonics and North American plate motions. *American Journal of Science*, *272*, 603–628. https://doi.org/10.2475/ajs.272.7.603

Cook, F. A., Clowes, R. M., Snyder, D. B., van der Velden, A. J., Hall, K. W., Erdmer, P., & Evenchick, C. A. (2004). Precambrian crust beneath the Mesozoic northern Canadian Cordillera discovered by Lithoprobe seismic reflection profiling. *Tectonics*, *23*, TC2010. https://doi.org/10.1029/2002TC001412

Cordey, F. (2020). Timing of Cache Creek ocean closure: Insights from new Jurassic radiolarian ages in British Columbia and Yukon and their significance for Canadian Cordillera tectonics. *Canadian Journal of Earth Sciences*, *57*, 1167–1179. https://doi.org/10.1139/cjes-2019-0236

Cordey, F., Gordey, S. P., & Orchard, M. J. (1991). New biostratigraphic data for the northern Cache Creek terrane, Teslin map area, southern Yukon. In *Current research*, Part E (paper 91-1E, pp. 67–76). Geological Survey of Canada.

Creaser, R. A., Erdmer, P., Stevens, R. A., & Grant, S. L. (1997). Tectonic affinity of Nisutlin and Anvil assemblage strata from the Teslin tectonic zone, northern Canadian Cordillera: Constraints from neodymium isotope and geochemical evidence. *Tectonics*, *16*, 107–121. https://doi.org/10.1029/96TC03317

Creaser, R. A., Goodwin-Bell, J. S., & Erdmer, P. (1999). Geochemical and Nd isotopic constraints for the origin of eclogite protoliths, northern Cordillera: Implications for the Paleozoic tectonic evolution of the Yukon-Tanana terrane. *Canadian Journal of Earth Sciences*, *36*, 1697–1709. https://doi.org/10.1139/e99-070

Creaser, R. A., Heaman, L. M., & Erdmer, P. (1997). Timing of high-pressure metamorphism in the Yukon-Tanana terrane, Canadian Cordillera: Constraints from U-Pb zircon dating of eclogite from the Teslin tectonic zone. *Canadian Journal of Earth Sciences*, *34*, 709–715. https://doi.org/10.1139/e17-057

Cui, Y., Miller, D., Schiarizza, P., & Diakow, L. J., & British Columbia Ministry of Energy, Mines and Petroleum Resources. (2017). *British Columbia digital geology* (open file 2017-8). British Columbia Geological Survey.

Currie, L. D. (1994). *The geology and mid-Jurassic amalgamation of Tracy Arm terrane and Stikinia of northwestern British Columbia* (PhD thesis). Carleton University.

Currie, L. D., & Parrish, R. R. (1993). Jurassic accretion of Nisling terrane along the western margin of Stikinia, Coast mountains, northwestern British Columbia. *Geology*, *21*, 235–238. https://doi.org/10.1130/0091-7613(1993)021<0235:JAONTA>2.3.CO;2

Davies, J. H., & von Blanckenburg, F. (1995). Slab breakoff: A model of lithosphere detachment and its test in the magmatism and deformation of collisional orogens. *Earth and Planetary Science Letters*, *129*, 85–102. https://doi.org/10.1016/0012-821X(94)00237-S

Dehkordi, B. H., Ferguson, I. J., Jones, A. G., & Ledo, J. (2019). Tectonics of the northern Canadian Cordillera imaged using modern magnetotelluric analysis. *Tectonophysics*, *765*, 102–128. https://doi.org/10.1016/j.tecto.2019.05.012

Diakow, L. J., Panteleyev, A., & Schroeter, T. G. (1993). *Geology of the early Jurassic Toodoggone Formation and gold-silver deposits in the Toodoggone River map area, northern British Columbia (Bulletin 86)*. British Columbia Ministry of Energy, Mines and Petroleum Tesources, British Columbia Geological Survey.

Diakow, L. J., & Rhodes, R. (2006). Geology between the Toodoggone River and Chukachida Lake (parts of NTS 94E/6, 7, 10 and 11), north-central British Columbia. In *Geological fieldwork 2005* (paper 2006-1, pp. 29–38). British Columbia Ministry of Energy, Mines and Petroleum Resources, British Columbia Geological Survey.

Dickie, J. R., & Hein, F. J. (1995). Conglomeratic fan deltas and submarine fans of the Jurassic Laberge Group, Whitehorse trough, Yukon Territory, Canada – Fore-arc sedimentation and unroofing of a volcanic island-arc complex. *Sedimentary Geology*, *98*, 263–292. https://doi.org/10.1016/0037-0738%2895%2900036-8

Dickinson, W. R. (2004). Evolution of the north American Cordillera. *Annual Reviews of Earth and Planetary Sciences*, *32*, 13–45. https://doi.org/10.1146/annurev.earth.32.101802.120257

Dostal, J., Church, B. N., & Hoy, T. (2001). Geological and geochemical evidence for variable magmatism and tectonics in the southern Canadian Cordillera: Paleozoic to Jurassic suites, Greenwood, southern British Columbia. *Canadian Journal of Earth Sciences*, *38*, 75–90. https://doi.org/10.1139/cjes-38-1-75

Dostal, J., Gale, V., & Church, B. N. (1999). Upper Triassic Takla group volcanic rocks, Stikine terrane, north-central British Columbia: Geochemistry, petrogenesis, and tectonic implications. *Canadian Journal of Earth Sciences*, *36*, 1483–1494. https://doi.org/10.1139/cjes-36-9-1483

Draut, A. E., & Clift, P. D. (2012). Basins in arc-continent collisions. In C. Busby, & A. Azor (Eds.), *Tectonics of sedimentary basins: Recent advances* (pp. 347–368). Blackwell Publishing.

Dusel-Bacon, C., Aleinikoff, J. N., Day, W. C., & Mortensen, J. K. (2015). Mesozoic magmatism and timing of epigenetic Pb-Zn-Ag mineralization in the western Fortymile mining district, east-central Alaska: Zircon U-Pb geochronology, whole-rock geochemistry, and Pb isotopes. *Geosphere*, *11*, 786–822. https://doi.org/10.1130/GES01092.1

Dyer, S. (2020). *The Early Jurassic metamorphic history of the Yukon-Tanana terrane of northwestern British Columbia: Insights from a new inverse garnet fractionation modelling technique* (master's thesis). Carleton University.

English, J. M., Johannson, G. G., Johnston, S. T., Mihalynuk, M. G., Fowler, M., & Wight, K. L. (2005). Structure, stratigraphy and petroleum resource potential of the central Whitehorse trough, northern Canadian Cordillera. *Bulletin of Canadian Petroleum Geology*, *53*, 130–153. https://doi.org/10.2113/53.2.130

Erdmer, P., Ghent, E. D., Archibald, D. A., & Stout, M. Z. (1998). Paleozoic and Mesozoic high-pressure metamorphism at the margin of ancestral North America in central Yukon. *Geological Society of America Bulletin*, *110*, 615–629. https://doi.org/10.1130/0016-7606(1998)110<0615:PAMHPM>2.3.CO;2

Evenchick, C. A. (1988). *Stratigraphy, metamorphism, structure, and their tectonic implications in the Sifton and Deserters ranges, Cassiar and northern Rocky mountains, northern British Columbia* (Bulletin 376). Geological Survey of Canada.

Evenchick, C. A., McMechan, M. E., McNicoll, V. J., & Carr, S. D. (2007). A synthesis of the Jurassic–Cretaceous tectonic evolution of the central and southeastern Canadian Cordillera: Exploring links across the orogen. In J. W. Sears, T. A. Harms, & C. A. Evenchick (Eds.), *Whence the mountains? Inquiries into the evolution of orogenic systems: A volume in honor of Raymond A. Price, special paper* (Vol. 433, pp. 117–145). Geological Society of America.

Evenchick, C. A., Poulton, T. P., & McNicoll, V. J. (2010). Nature and significance of the diachronous contact between the Hazelton and Bowser Lake groups (Jurassic), north-central British Columbia. *Bulletin of Canadian Petroleum Geology*, *58*, 235–267. https://doi.org/10.2113/gscpgbull.58.3.235

Ferri, F. (1997). Nina Creek group and Lay Range assemblage, north-central British Columbia: Remnants of late Paleozoic oceanic and arc terranes. *Canadian Journal of Earth Sciences*, *34*, 854–874. https://doi.org/10.1139/e17-070

Frazer, R. E., Coleman, D. S., & Mills, R. D. (2014). Zircon U-Pb geochronology of the Mount Givens Granodiorite: Implications for genesis of large volumes of eruptible magma. *Journal of Geophysical Research: Solid Earth*, *119*, 2907–2924. https://doi.org/10.1002/2013JB010716

Gabrielse, H. (1985). Major dextral transcurrent displacements along the northern Rocky Mountain Trench and related lineaments in north-central British Columbia. *Geological Society of America Bulletin*, *96*, 1–14. https://doi.org/10.1130/0016-7606(1985)96<1:MDTDAT>2.0.CO;2

Gabrielse, H. (1998). *Geology of Cry Lake and Dease Lake map areas, north-central British Columbia* (Bulletin 504). Geological Survey of Canada.

Gabrielse, H., Murphy, D. C., & Mortensen, J. K. (2006). Cretaceous and Cenozoic dextral orogen-parallel displacements, magmatism and paleogeography, north-central Canadian Cordillera. In J. W. Haggart, J. W. H. Monger, & R. J. Enkin (Eds.), *Paleogeography of the north American Cordillera: Evidence for and against large-scale displacements, special paper* (Vol. 46, pp. 255–276). Geological Association of Canada.

Gagnon, J.-F., Baressi, T., Waldron, J. W. F., Nelson, J. L., Poulton, T. P., & Cordey, F. (2012). Stratigraphy of the upper Hazelton group and the Jurassic evolution of the Stikine terrane, British Columbia. *Canadian Journal of Earth Sciences*, *49*, 1027–1052. https://doi.org/10.1139/e2012-042

Gagnon, J.-F., Evenchick, C. A., Waldron, J. W. F., Cordey, F., & Poulton, T. P. (2009). Jurassic subsidence history of the Hazelton trough - Bowser basin in the area of Todagin mountain, north-central British Columbia, Canada. *Bulletin of Canadian Petroleum Geology*, *57*, 430–448. https://doi.org/10.2113/gscpgbull.57.4.430

Gaidies, F., Morneau, Y. E., Petts, D. C., Jackson, S. E., Zagorevski, A., & Ryan, J. J. (2021). Major and trace element mapping of garnet: Unravelling the conditions, timing and rates of metamorphism of the Snowcap assemblage, west-central Yukon. *Journal of Metamorphic Geology*, *39*, 133–164. https://doi.org/10.1111/jmg.12562

George, S. W. M., Nelson, J. L., Alberts, D., Greig, C. J., & Gehrels, G. E. (2021). Triassic–Jurassic accretionary history and tectonic origins of Stikinia from U-Pb geochronology and Lu-Hf isotope analysis, British Columbia. *Tectonics*, *40*, e2020TC006505. https://doi.org/10.1029/2020TC006505

Gilotti, J. A., McClelland, W. C., van Staal, C. R., & Petrie, M. B. (2017). Detrital zircon evidence for eclogite formation by basal subduction erosion – An example from the Yukon-Tanana composite arc, Canadian Cordillera. In G. Bianchini, J.-L. Bodinier, R. Braga, & M. Wilson

(Eds.), *The crust-mantle and lithosphere-asthenosphere boundaries: Insights from xenoliths, orogenic deep sections, and geophysical studies, special paper* (Vol. 526, pp. 173–189). Geological Society of America.

Glazner, A. F., Bartley, J. M., Coleman, D. S., Gray, W., & Taylor, R. Z. (2004). Are plutons assembled over millions of years by amalgamation from small magma chambers? *Geological Society of America Today*, *14*(4/5), 4–11. https://doi.org/10.1130/1052-5173(2004)0142.0.CO;2

Golding, M. L., Mortensen, J. K., Ferri, F., Zonneveld, J.-P., & Orchard, M. J. (2016). Determining the provenance of Triassic sedimentary rocks in northeastern British Columbia and western Alberta using detrital zircon geochronology, with implications for regional tectonics. *Canadian Journal of Earth Sciences*, *53*, 140–155. https://doi.org/10.1139/cjes-2015-0082

Gordey, S. P., & Makepeace, A. J. (2001). *Bedrock geology, Yukon Territory* (open file 3754). Geological Survey of Canada.

Greig, C. J. (2014). Latest Triassic-earliest Jurassic contractional deformation, uplift and erosion in Stikinia, NW B.C. In *Annual meeting, abstracts with programs* (Vol. 46, pp. 588). Geological Society of America.

Greig, C. J., & Gehrels, G. E. (1995). U-Pb zircon geochronology of lower Jurassic and Paleozoic Stikinian strata and Tertiary intrusions, northwestern British Columbia. *Canadian Journal of Earth Sciences*, *32*, 1155–1171. https://doi.org/10.1139/e95-095

Gunning, M. H., Hodder, R. W. H., & Nelson, J. L. (2006). Contrasting volcanic styles and their tectonic implications for the Paleozoic Stikine assemblage, western Stikine terrane, northwestern British Columbia. In M. Colpron, & J. L. Nelson (Eds.), *Paleozoic evolution and metallogeny of pericratonic terranes at the Ancient Pacific Margin of North America, Canadian and Alaskan Cordillera, special paper* (Vol. 45, pp. 201–227). Geological Association of Canada.

Hammarstrom, J. M., & Zen, E. A. (1986). Aluminum in hornblende: An empirical igneous geobarometer. *American Mineralogist*, *71*, 1297–1313. Retrieved from https://pubs.geoscienceworld.org/msa/ammin/article-abstract/71/11-12/1297/104900/Aluminum-in-hornblende-An-empirical-igneous

Han, T., Ootes, L., & Yun, K. (2020). *The new British Columbia geological Survey geochronologic database: Preliminary release of ages* (GeoFile 2020-10). British Columbia Ministry of Energy, Mines and Petroleum Resources, British Columbia Geological Survey.

Harris, M. J., Symons, D. T. A., Blackburn, W. H., Hart, C. J. R., & Villeneuve, M. E. (2003). Travels of the Cache Creek terrane: A paleomagnetic, geobarometric and $^{40}Ar/^{39}Ar$ study of the Fourth of July Batholith, Canadian Cordillera. *Tectonophysics*, *362*, 137–159. Retrieved from https://www.sciencebase.gov/catalog/item/5771b8c5e4b07657d1a6d212

Hart, C. J. R. (1995). *Magmatic and tectonic evolution of the Intermontane superterrane and Coast Plutonic complex in southern Yukon Territory* (master's thesis). University of British Columbia.

Hart, C. J. R. (1997). *A transect across northern Stikinia: Geology of the northern Whitehorse map area, southern Yukon Territory (105D/13-16)*, (Bulletin 8). Yukon Geological Survey.

Hart, C. J. R., Dickie, J. R., Ghosh, D. K., & Armstrong, R. L. (1995). Provenance constraints for Whitehorse trough conglomerate: U-Pb zircon dates and initial Sr ratios of granitic clasts in Jurassic Laberge Group, Yukon Territory. In D. M. Miller, & C. Busby (Eds.), *Jurassic magmatism and tectonics of the North American Cordillera, special paper* (Vol. 299, pp. 47–63). Geological Society of America.

Hodges, K. (2014). Thermochronology in orogenic systems. In H. D. H. K. Turekian (Ed.), *Treatise on geochemistry* (2nd ed., pp. 281–308). Elsevier.

Jackson, J. L., Gehrels, G. E., Patchett, P. J., & Mihalynuk, M. G. (1991). Stratigraphy and isotopic link between the northern Stikine terrane and an ancient continental margin assemblage, Canadian Cordillera. *Geology*, *19*, 1177–1180. https://doi.org/10.1130/0091-7613(1991)019<1177:SAILBT>2.3.CO;2

Johannson, G. G., Smith, P. L., & Gordey, S. P. (1997). Early Jurassic evolution of the northern Stikinian arc: Evidence from the Laberge group, northwestern British Columbia. *Canadian Journal of Earth Sciences*, *34*, 1030–1057. https://doi.org/10.1139/e17-085

Jones, G., Ootes, L., Milidragovic, D., Friedman, R., Camacho, A., Luo, Y., et al. (2021). Geochronology of northern Hogem batholith, Quesnel terrane, north-central British Columbia. In *Geological fieldwork 2020* (Paper 2021-1, pp. 37–56). British Columbia Ministry of Energy, Mines and Low Carbon Innovation, British Columbia Geological Survey.

Joyce, N. L., Ryan, J. J., Colpron, M., Hart, C. J. R., & Murphy, D. C. (2015). *A compilation of $^{40}Ar/^{39}Ar$ age determinations for igneous and metamorphic rocks, and mineral occurrences from central and southeast Yukon* (open file 7924). Geological Survey of Canada.

Kay, R. W., & Kay, S. M. (1993). Delamination and delamination magmatism. *Tectonophysics*, *219*, 177–189. https://doi.org/10.1016/0040-1951(93)90295-U

Kellett, D. A., & Iraheta Muniz, P. (2019). *Detrital U-Pb zircon and $^{40}Ar/^{39}Ar$ muscovite geochronology of the Whitehorse trough, and surrounding rocks, Yukon and British Columbia* (open file 8565). Geological Survey of Canada.

Kellett, D. A., Weller, O. M., Zagorevski, A., & Regis, D. (2018). A petrochronological approach for the detrital record: Tracking mm-sized eclogite clasts in the northern Canadian Cordillera. *Earth and Planetary Science Letters*, *494*, 23–31. https://doi.org/10.1016/j.epsl.2018.04.036

Kent, D. V., & Irving, E. (2010). Influence of inclination error in sedimentary rocks on the Triassic and Jurassic apparent pole wander path for North America and implications for Cordilleran tectonics. *Journal of Geophysical Research*, *115*, 1–25. https://doi.org/10.1029/2009JB007205

Klöcking, M., Mills, L., Mortensen, J. K., & Roots, C. F. (2016). *Geology of mid-Cretaceous volcanic rocks at Mount Nansen, central Yukon, and their relationship to the Dawson Range batholith* (open file 2016-25). Yukon Geological Survey.

Knight, E., Schneider, D. A., & Ryan, J. J. (2013). Thermochronology of the Yukon-Tanana terrane, west-central Yukon: Evidence for Jurassic extension and exhumation in the northern Cordillera. *The Journal of Geology*, *121*, 371–400. https://doi.org/10.1086/670721

Kovacs, N., Allan, M. M., Crowley, J. L., Colpron, M., Hart, C. J. R., Zagorevski, A., & Creaser, R. A. (2020). Carmacks copper Cu-Au-Ag deposit: Mineralization and post-ore migmatization of a Stikine arc porphyry copper system in Yukon, Canada. *Economic Geology*, *115*, 1413–1442. https://doi.org/10.5382/econgeo.4756

Labails, C., Olivet, J.-L., Aslanian, D., & Roest, W. R. (2010). An alternative early opening scenario for the Central Atlantic Ocean. *Earth and Planetary Science Letters*, *297*, 355–368. https://doi.org/10.1016/j.epsl.2010.06.024

Le Bas, M. J., Le Maitre, R. W., Streckeisen, A., & Zanettin, B. (1986). A chemical classification of volcanic rocks based on the total alkalis-silica diagram. *Journal of Petrology*, *27*, 745–750. https://doi.org/10.1093/petrology/27.3.745

Le Bas, M. J., & Streckeisen, A. L. (1991). The IUGS systematics of igneous rocks. *Journal of the Geological Society*, *148*, 825–833.

Logan, J. M., Drobe, J. R., & McClelland, W. C. (2000). *Geology of the Forrest Kerr – Mess Creek area, northwestern British Columbia (NTS 104B/10, 15 & 104G/2 & 7W)* (Bulletin 104). British Columbia Ministry of Energy and Mines, British Columbia Geological Survey.

Logan, J. M., & Mihalynuk, M. G. (2014). Tectonic controls on Early Mesozoic paired alkaline porphyry deposit belts (Cu-Au ± Ag-Pt-Pd-Mo) within the Canadian Cordillera. *Economic Geology*, *109*, 827–858. https://doi.org/10.2113/econgeo.109.4.827

Logan, J. M., Moynihan, D. P., & Diakow, L. J. (2012). *Dease Lake Geoscience Project, Part I: Geology and mineralization of the Dease Lake (NTS 104J/08) and east-half of the Little Tuya River (NTS 104J/07E) map sheets, northern British Columbia*, *Geological Fieldwork 2011* (Paper 2012-1, pp. 23–44). British Columbia Ministry of Energy, Mines and Petroleum Resources, British Columbia Geological Survey.

Long, D. G. F. (2015). *Depositional and tectonic framework of braided and meandering gravel-bed river deposits and associated coal deposits in active intermontane basins: The Upper Jurassic to mid-Cretaceous Tantalus Formation, Whitehorse trough* (open file 2015-23). Yukon Geological Survey.

Lowey, G. W. (2008). Summary of the stratigraphy, sedimentology and hydrocarbon potential of the Laberge group (Lower-Middle Jurassic), Whitehorse trough, Yukon. In D. S. Emond, L. R. Blackburn, R. P. Hill, & L. H. Weston (Eds.), *Yukon exploration and geology 2007* (pp. 179–197). Yukon Geological Survey.

Marsden, H., & Thorkelson, D. J. (1992). Geology of the Hazelton volcanic belt in British Columbia: Implications for the early to Middle Jurassic evolution of Stikinia. *Tectonics*, *11*, 1266–1287. https://doi.org/10.1029/92TC00276

McCartney, T. M. (2012). *A methodology for studying tectonic subsidence variations: Insight from the Fernie Formation of west-central Alberta* (master's thesis). University of Calgary.

McCausland, P. J. A., Symons, D. T. A., Hart, C. J. R., & Blackburn, W. H. (2002). Paleomagnetism and geobarometry of the granite mountain batholith, Yukon: Minimal geotectonic motion of the Yukon-Tanana terrane relative to north America. In D. S. Emond, L. H. Weston, & L. L. Lewis (Eds.), *Yukon exploration and geology 2001*. (pp. 163–177). Yukon Geological Survey.

McGoldrick, S., Zagorevski, A., & Canil, D. (2017). Geochemistry of volcanic and plutonic rocks from the Nahlin ophiolite with implications for a Permo-Triassic arc in the Cache Creek terrane, northwestern British Columbia. *Canadian Journal of Earth Sciences*, *54*, 1214–1227. https://doi.org/10.1139/cjes-2017-0069

Mihalynuk, M. G., Erdmer, P., Ghent, E. D., Cordey, F., Archibald, D. A., Friedman, R. M., & Johannson, G. G. (2004). Coherent French Range blueschist: Subduction to exhumation in <2.5 m.y. *Geological Society of America Bulletin*, *116*, 910–922. https://doi.org/10.1130/B25393

Mihalynuk, M. G., Mountjoy, K. J., Smith, M. T., Currie, L. D., Gabites, J. E., Tipper, H. W., et al. (1999). *Geology and mineral resources of the Tagish Lake area (NTS 104M/8, 9, 10E, 15 and 104N/12W), northwestern British Columbia* (Bulletin 105). British Columbia Ministry of Energy and Mines, British Columbia Geological Survey.

Mihalynuk, M. G., Nelson, J., & Diakow, L. J. (1994). Cache Creek terrane entrapment: Oroclinal paradox within the Canadian Cordillera. *Tectonics*, *13*, 575–595. https://doi.org/10.1029/93TC03492

Mihalynuk, M. G., Smith, M. T., Gabites, J. E., Runkle, D., & Lefebure, D. (1992). Age of emplacement and basement character of the Cache Creek terrane as constrained by new isotopic and geochemical data. *Canadian Journal of Earth Sciences*, *29*, 2463–2477. https://doi.org/10.1139/e92-193

Mihalynuk, M. G., Zagorevski, A., Milidragovic, D., Tsekhmistrenko, M., Friedman, R. M., Joyce, N., et al. (2018). Geologic and geochronologic update of the Turtle Lake area, NTS 104M/16, northwest British Columbia. In *Geological fieldwork 2017*. (Paper 2018-1, pp. 83–128). British Columbia Ministry of Energy, Mines and Petroleum Resources, British Columbia Geological Survey.

Monger, J. W. H. (1977). Upper Paleozoic rocks of the western Canadian Cordillera and their bearing on Cordilleran evolution. *Canadian Journal of Earth Sciences*, *14*, 1832–1859. https://doi.org/10.1139/e77-156

Monger, J. W. H., & Gibson, H. D. (2019). Mesozoic-cenozoic deformation in the Canadian Cordillera: The record of a "Continental Bulldozer". *Tectonophysics*, *757*, 153–169. https://doi.org/10.1016/j.tecto.2018.12.023

Monger, J. W. H., & Nokleberg, W. J. (1996). Evolution of the northern north American Cordillera: Generation, fragmentation, displacement and accretion of successive north American plate-margin arcs. In A. R. Coyner, & P. L. Fahey (Eds.), *Geology and ore deposits of the American Cordillera symposium proceedings* (III, 1133–1152). Geological Society of Nevada.

Monger, J. W. H., & Price, R. A. (2002). The Canadian Cordillera: Geology and tectonic evolution. *Canadian Society of Exploration Geophysicists Recorder*, *27*, 17–36.

Monger, J. W. H., Price, R. A., & Tempelman-Kluit, D. J. (1982). Tectonic accretion and the origin of two metamorphic and plutonic welts in the Canadian Cordillera. *Geology*, *10*, 70–75. https://doi.org/10.1130/0091-7613(1982)10<70:TAATOO>2.0.CO;2

Monger, J. W. H., & Ross, C. A. (1971). Distribution of fusulinaceans in the western Canadian Cordillera. *Canadian Journal of Earth Sciences*, *8*, 259–278. https://doi.org/10.1139/e71-026

Mortensen, J. K. (1990). Geology and U-Pb geochronology of the Klondike district, west-central Yukon. *Canadian Journal of Earth Sciences*, *27*, 903–914. https://doi.org/10.1139/e90-093

Mortensen, J. K. (1992). Pre-Mid-Mesozoic tectonic evolution of the Yukon-Tanana terrane, Yukon and Alaska. *Tectonics*, *11*, 836–853. https://doi.org/10.1029/91TC01169

Mortensen, J. K., Ghosh, D., & Ferri, F. (1995). U-Pb age constraints of intrusive rocks associated with copper-gold porphyry deposits in the Canadian Cordillera. In T. G. Schroeter (Ed.), *Porphyry deposits of the northwestern Cordillera of North America*, *Special Volume* (Vol. 46, pp. 142–158). Canadian Institute of Mining and Metallurgy.

Mortensen, J. K., & Jilson, G. A. (1985). Evolution of the Yukon-Tanana terrane: Evidence from southeastern Yukon Territory. *Geology*, *13*, 806–810. https://doi.org/10.1130/0091-7613(1985)13<806:EOTYTE>2.0.CO;2

Murphy, D. C., van der Heyden, P., Parrish, R. R., Klepacki, D. W., McMillan, W., Struik, L. C., & Gabites, J. (1995). New geochronological constraints on Jurassic deformation of the western edge of North America, southeastern Canadian Cordillera. In D. M. Miller, & C. Busby (Eds.), *Jurassic magmatism and tectonics of the North American Cordillera, special paper* (Vol. 299, pp. 159–171). Geological Society of America.

Nelson, J. L., & Colpron, M. (2007). Tectonics and metallogeny of the Canadian and Alaskan Cordillera, 1.8 Ga to present. In W. D. Goodfellow (Ed.), *Mineral deposits of Canada: A synthesis of major deposit types, district metallogeny, the evolution of geological provinces, and exploration methods, special publication* (Vol. 5, pp. 755–791). Mineral Deposit Division, Geological Association of Canada.

Nelson, J. L., Colpron, M., & Israel, S. (2013). The Cordillera of British Columbia, Yukon, and Alaska: Tectonics and metallogeny. In M. Colpron, T. Bissig, B. G. Rusk, & J. F. H. Thompson (Eds.), *Tectonics, metallogeny and discovery: The North American Cordillera and similar accretionary settings*, *Special Publication* (Vol. 17, 53–103). Society of Economic Geologists.

Nelson, J. L., Colpron, M., Piercey, S. J., Dusel-Bacon, C., Murphy, D. C., & Roots, C. F. (2006). Paleozoic tectonic and metallogenic evolution of the pericratonic terranes in Yukon, northern British Columbia and eastern Alaska. In M. Colpron, & J. L. Nelson (Eds.), *Paleozoic evolution and metallogeny of pericratonic terranes at the Ancient Pacific Margin of North America, Canadian and Alaskan Cordillera, special paper* (Vol. 45, pp. 323–360). Geological Association of Canada.

Nelson, J. L., & Friedman, R. M. (2004). Superimposed Quesnel (late Paleozoic-Jurassic) and Yukon-Tanana (Devonian-Mississippian) arc assemblages, Cassiar mountains, northern British Columbia: Field, U-Pb and igneous petrochemical evidence. *Canadian Journal of Earth Sciences*, *41*, 1201–1235. https://doi.org/10.1139/e04-028

Nelson, J. L., & Mihalynuk, M. G. (1993). Cache Creek Ocean: Closure or enclosure? *Geology*, *21*, 173–176. https://doi.org/10.1130/0091-7613(1993)021<0173:CCOCOE>2.3.CO;2

Nelson, J. L., van Straaten, B., & Friedman, R. (2022). *Latest Triassic-Early Jurassic Stikine – Yukon-Tanana terrane collision and the onset of accretion in the Canadian Cordillera: Insights from Hazelton Group detrital zircon provenance and arc–back-arc configuration*. (In press). https://doi.org/10.1130/GES02444.1

Nelson, J. L., Waldron, J. W. F., van Straaten, B., Zagorevski, A., & Rees, C. J. (2018). Revised stratigraphy of the Hazelton Group in the Iskut River region, northwestern British Columbia. In *Geological fieldwork 2017* (Paper 2018-1, pp. 15–38). British Columbia Ministry of Energy, Mines and Petroleum Resources, British Columbia Geological Survey.

Nixon, G. T., Hammack, J. L., Ash, C. H., Cabri, L. J., Case, G., Connelly, J. N., et al. (1997). *Geology and platinum-group-element mineralization of Alaskan-type ultramafic-mafic complexes in British Columbia* (Bulletin 93). British Columbia Ministry of Energy and Mines, British Columbia Geological Survey.

Nixon, G. T., Scheel, J. E., Scoates, J. S., Friedman, R. M., Wall, C. J., Gabites, J., & Jackson-Brown, S. (2020). Syn-accretionary multistage assembly of an Early Jurassic Alaskan-type intrusion in the Canadian Cordillera: U-Pb and $^{40}Ar/^{39}Ar$ geochronology of the Turnagain ultramafic-mafic intrusive complex, Yukon-Tanana terrane. *Canadian Journal of Earth Sciences*, *57*, 575–600. https://doi.org/10.1139/cjes-2019-0121

Pană, D. I., Poulton, T. P., & DuFrane, S. A. (2018). U-Pb detrital zircon dating supports Early Jurassic initiation of the Cordilleran foreland basin in southwestern Canada. *Geological Society of America Bulletin*, *131*, 318–334. https://doi.org/10.1130/B31862.1

Parsons, A. J., Coleman, M. J., Ryan, J. J., Zagorevski, A., Joyce, N. L., Gibson, H. D., & Larson, K. P. (2018). Structural evolution of a crustal-scale shear zone through a decreasing temperature regime: The Yukon River shear zone, Yukon-Tanana terrane, Northern Cordillera. *Lithosphere*, *10*, 760–782. https://doi.org/10.1130/L724.1

Peccerillo, A., & Taylor, S. R. (1976). Geochemistry of calc-alkaline volcanic rocks from the Kastamonu area, Northern Turkey. *Contributions to Mineralogy and Petrology*, *58*, 63–81. https://doi.org/10.1007/BF00384745

Pecha, M. E., Gehrels, G. E., McClelland, W. C., Giesler, D., White, C., & Yokelson, I. (2016). Detrital zircon U-Pb geochronology and Hf isotope geochemistry of the Yukon-Tanana terrane, Coast Mountains, southeast Alaska. *Geosphere*, *12*, 1556–1574. https://doi.org/10.1130/GES01303.1

Petrie, M. B., Massonne, H.-J., Gilotti, J. A., McClelland, W. C., & van Staal, C. R. (2016). The P-T path of eclogite in the St. Cyr klippe, Yukon, Canada: Permian metamorphism of a coherent high-pressure unit in an accreted terrane of the North American Cordillera. *European Journal of Mineralogy*, *28*, 1111–1130. https://doi.org/10.1127/ejm/2016/0028-2576

Piercey, S. J., & Colpron, M. (2009). Composition and provenance of the Snowcap assemblage, basement to the Yukon-Tanana terrane, northern Cordillera: Implications for Cordilleran crustal growth. *Geosphere*, *5*, 439–464. https://doi.org/10.1130/GES00505.1

Piercey, S. J., Nelson, J. L., Colpron, M., Dusel-Bacon, C., Roots, C. F., & Simard, R.-L. (2006). Paleozoic magmatism and crustal recycling along the Ancient Pacific Margin of North America, northern Cordillera. In M. Colpron, & J. L. Nelson (Eds.), *Paleozoic evolution and metallogeny of pericratonic terranes at the Ancient Pacific Margin of North America, Canadian and Alaskan Cordillera, special paper* (Vol. 45, pp. 281–322). Geological Association of Canada.

Read, P. B., Woodsworth, G. J., Greenwood, H. J., Ghent, E. D., & Evenchick, C. A. (1991). *Metamorphic map of the Canadian Cordillera (map 1714A)*. Geological Survey of Canada.

Roots, C. F., Nelson, J. L., Mihalynuk, M. G., Harms, T. A., de Keijzer, M., & Simard, R.-L. (2004). *Bedrock geology, Dorsey Lake (NTS 105B/4), southern Yukon (1:50,000 scale)* (open file 2004-2). Yukon Geological Survey.

Roots, C. F., Nelson, J. L., Simard, R.-L., & Harms, T. A. (2006). Continental fragments, mid-Paleozoic arcs and overlapping late Paleozoic arc and Triassic sedimentary strata in the Yukon-Tanana terrane of northern British Columbia and southern Yukon. In M. Colpron, & J. L. Nelson (Eds.), *Paleozoic evolution and metallogeny of pericratonic terranes at the Ancient Pacific Margin of North America, Canadian and Alaskan Cordillera, special paper* (Vol. 45, pp. 153–177). Geological Association of Canada.

Ross, C. A., & Monger, J. W. H. (1978). Carboniferous and Permian fusulinaceans from the Omineca Mountains, British Columbia. In V. Donnelly (Ed.), *Contributions to Canadian paleontology* (Bulletin 267, pp. 43–63). Geological Survey of Canada.

Ross, C. A., & Ross, J. R. P. (1983). Late Paleozoic accreted terranes of western North America. In C. H. Stevens (Ed.), *Pre-Jurassic rocks in western North American suspect terranes* (pp. 7–22). Society of Economic Paleontologists and Mineralogists.

Rudnick, R. L. (1995). Making continental crust. *Nature*, *378*, 571–578. https://doi.org/10.1038/378571a0

Ruks, T. W., Piercey, S. J., Ryan, J. J., Villeneuve, M. E., & Creaser, R. A. (2006). Mid- to late Paleozoic K-feldspar augen granitoids of the Yukon-Tanana terrane, Yukon, Canada: Implications for crustal growth and tectonic evolution of the northern Cordillera. *Geological Society of America Bulletin*, *118*, 1212–1231. https://doi.org/10.1130/B25854.1

Ryan, J. J., Zagorevski, A., Roots, C. F., & Joyce, N. (2014). *Paleozoic tectonostratigraphy of the northern Stevenson Ridge area, Yukon* (current research 2014-4). Geological Survey of Canada.

Ryan, J. J., Zagorevski, A., Williams, S. P., Roots, C. F., Ciolkiewicz, W., Hayward, N., & Chapman, J. B. (2013). *Geology, Stevenson Ridge (northeast part), Yukon (Canadian geoscience map 116)*. Geological Survey of Canada.

Sack, P. J., Colpron, M., & Crowley, J. L. (2022). *U-Pb zircon geochronology from a Late Triassic pluton in the Mount Nansen area* (open file 2022-2). Yukon Geological Survey. https://data.geology.gov.yk.ca/Reference/95925

Sack, P. J., Colpron, M., Crowley, J. L., Ryan, J. J., Allan, M. M., Beranek, L. P., et al. (2020). *Atlas of Late Triassic to Jurassic plutons in the Intermontane terranes of Yukon* (open file 2020-1). Yukon Geological Survey. http://data.geology.gov.yk.ca/Reference/95839

Schellart, W. P., Freeman, J., Stegman, D. R., & May, D. (2007). Evolution and diversity of subduction zones controlled by slab width. *Nature*, *446*, 308–311. https://doi.org/10.1038/nature05615

Schiarizza, P. (2012). *Geology of the Kutcho assemblage between the Kehlechoa and Tucho Rivers, northern British Columbia (NTS 104I/01, 02), geological fieldwork 2011* (Paper 2012-1, pp. 75–98). British Columbia Ministry of Energy, Mines and Petroleum Resources, British Columbia Geological Survey.

Schmidt, M. W., & Poli, S. (2004). Magmatic epidote. In A. Liebscher, & G. Franz (Eds.), *Epidotes. Reviews in mineralogy and geochemistry* (Vol. 56, pp. 399–430). Mineralogical Society of America.

Schneider, C. A., Rasband, W. S., & Eliceiri, K. W. (2012). NIH Image to ImageJ: 25 years of image analysis. *Nature Methods*, *9*, 671–675. https://doi.org/10.1038/nmeth.2089

Schwartz, J. J., Klepeis, K. A., Sadorski, J. F., Stowell, H. H., Tulloch, A. J., & Coble, M. A. (2017). The tempo of continental arc construction in the Mesozoic Median Batholith, Fiordland, New Zealand. *Lithosphere*, *9*, 343–365. https://doi.org/10.1130/L610.1

Shand, S. J. (1943). *Eruptive rocks; their genesis, composition, classification, and their relation to ore deposits, with a chapter on meteorites* (444 p.). Hafner Publishing Co.

Shirmohammad, F., Smith, P. L., Anderson, R. G., & McNicoll, V. J. (2011). The Jurassic succession at Lisadele Lake (Tulsequah map area, British Columbia, Canada) and its bearing on the tectonic evolution of the Stikine terrane. *Volumina Jurassica*, *9*, 43–60. Retrieved from http://31.186.81.235:8080/api/files/view/36878.pdf

Simard, R.-L. (2003). *Geological map of southern Semenof Hills (part of NTS 105E/1,7,8), south-central Yukon (1:50 000 scale)* (open file 2003-12). Yukon Geological Survey.

Simard, R.-L., & Devine, F. (2003). Preliminary geology of the southern Semenof Hills, central Yukon (105E/1,7,8). In D. S. Emond, & L. L. Lewis (Eds.), *Yukon exploration and geology 2002* (pp. 213–222). Yukon Geological Survey.

Simard, R.-L., Dostal, J., & Roots, C. F. (2003). Development of late Paleozoic volcanic arcs in the Canadian Cordillera: An example from the Klinkit Group, northern British Columbia and southern Yukon. *Canadian Journal of Earth Sciences*, *40*, 907–924. https://doi.org/10.1139/e03-025

Smith, P. L. (2006). Paleobiogeography and Early Jurassic molluscs in the context of terrane displacement in western Canada. In J. W. Haggart, R. J. Enkin, & J. W. H. Monger (Eds.), *Paleogeography of the North American Cordillera: Evidence for and against large-scale displacements. Special paper* (Vol. 46, pp. 81–94). Geological Association of Canada.

Smith, P. L., Tipper, H. W., & Ham, D. M. (2001). Lower Jurassic Amaltheidae (Ammotina) in North America: Paleobiogeography and tectonic implications. *Canadian Journal of Earth Sciences*, *38*, 1439–1449. https://doi.org/10.1139/e01-034

Smith, T., Rosenbaum, G., & Gross, L. (2021). Formation of oroclines by buckling continental ribbons: Fact or fiction? *Tectonophysics*, *814*, 9. https://doi.org/10.1016/j.tecto.2021.228950

Souther, J. G. (1971). *Geology and mineral deposits of Tulsequah map-area, British Columbia*, (Memoir 362). Geological Survey of Canada.

Stanley, G. D. J., & Senowbari-Daryan, B. (1999). Upper Triassic reef fauna from the Quesnel terrane, central British Columbia, Canada. *Journal of Paleontology*, *73*, 787–802. Retrieved from https://www.mindat.org/taxon-P70336.html

Staples, R. D., Gibson, H. D., Colpron, M., & Ryan, J. J. (2016). An orogenic wedge model for diachronous deformation, metamorphism, and exhumation in the hinterland of the northern Canadian Cordillera. *Lithosphere*, *8*, 165–184. https://doi.org/10.1130/L472.1

Stevens, C. H. (1995). A giant Permian fusulinid from east-central Alaska with comparisons of all giant fusulinids in western North America. *Journal of Paleontology*, *69*, 802–812. https://doi.org/10.1017/S0022336000035484

Sundell, K., Saylor, J. E., & Pecha, M. (2019). Provenance and recycling of detrital zircons from Cenozoic Altiplano strata and the crustal evolution of western South America from combined U-Pb and Lu-Hf isotopic analysis. In B. K. Horton, & A. Folguera (Eds.), *Andean tectonics* (pp. 363–397). Elsevier.

Tafti, R. (2005).*Nature and origin of the early Jurassic Copper (-Gold) deposits at Minto and Williams Creek, Carmacks Copper belt, western Yukon: Examples of deformed porphyry deposits* (master's thesis). University of British Columbia.

Tempelman-Kluit, D. J. (1984). *Geology, Laberge (105E) and Carmacks (105I), Yukon Territory* (open file 1101). Geological Survey of Canada.

Tempelman-Kluit, D. J. (2009). *Geology of Carmacks and Laberge map areas, central Yukon: Incomplete draft manuscript on stratigraphy, structure and its early interpretation (ca. 1986)*. (open file 5982). Geological Survey of Canada.

Tipper, H. W. (1978). Jurassic biostratigraphy, Cry Lake map area, British Columbia. In *Current Research* (Paper 78-1A, pp. 25–27). Geological Survey of Canada.

Tipper, H. W., & Richards, T. A. (1976). *Jurassic stratigraphy and history of north-central British Columbia*, (Bulletin 270). Geological Survey of Canada.

Topham, M. J., Allan, M. M., Mortensen, J. K., Hart, C. J. R., Colpron, M., & Sack, P. J. (2016). Crustal depth of emplacement of the Early Jurassic Aishihik and Tatchun batholiths, west-central Yukon. In K. E. MacFarlane, & M. G. Nordling (Eds.), *Yukon exploration and geology 2015* (pp. 233–251). Yukon Geological Survey.

Travers, W. B. (1978). Overturned Nicola and Ashcroft strata and their relation to the Cache Creek Group, southwestern Intermontane Belt, British Columbia. *Canadian Journal of Earth Sciences*, *15*, 99–116. https://doi.org/10.1139/e78-009

Unterschutz, J. L. E., Creaser, R. A., Erdmer, P., Thompson, R. I., & Daughtry, K. L. (2002). North American margin origin of Quesnel terrane strata in the southern Canadian Cordillera: Inferences from geochemical and Nd isotopic characteristics of Triassic metasedimentary rocks. *Geological Society of America Bulletin*, *114*, 462–475. https://doi.org/10.1130/0016-7606(2002)114<0462:NAMOOQ>2.0.CO;2

van Drecht, L. (2019). *Detrital zircon U-Pb geochronology and Hf isotope geochemistry of the Laberge Group: Synorogenic siliciclastic record of early Mesozoic crustal thickening and tectonic evolution of the Whitehorse trough in the northern Canadian Cordillera* (master's thesis). Memorial University of Newfoundland.

Vervoot, J. D., Patchett, P. J., Blichert-Toft, J., & Albarède, F. (1999). Relationships between Lu-Hf and Sm-Nd isotopic systems in the global sedimentary system. *Earth and Planetary Science Letters*, *168*, 79–99. https://doi.org/10.1016/S0012-821X(99)00047-3

von Blanckenburg, F., & Davies, J. H. (1995). Slab breakoff: A model for syncollisional magmatism and tectonics in the Alps. *Tectonics*, *14*, 120–131. https://doi.org/10.1029/94TC02051

Wernicke, B., & Klepacki, D. W. (1988). Escape hypothesis for the Stikine block. *Geology*, *16*, 461–464. https://doi.org/10.1130/0091-7613(1988)016<0461:EHFTSB>2.3.CO;2

Wheeler, J. O. (1961). *Whitehorse map-area, Yukon Territory, 105D* (Memoir 312). Geological Survey of Canada.

Wheeler, J. O., & McFeely, P. (1991). *Tectonic assemblage map of the Canadian Cordillera and adjacent parts of the United States of America (Map 1712A)*. Geological Survey of Canada.

White, D., Colpron, M., & Buffett, G. (2012). Seismic and geological constraints on the structure of the northern Whitehorse trough, Yukon, Canada. *Bulletin of Canadian Petroleum Geology*, *60*, 239–255. https://doi.org/10.2113/gscpgbull.60.4.239

Wilson, F. H., Hults, C. P., Mull, C. G., & Karl, S. M. (2015). *Geologic map of Alaska (scientific investigation map 3340)*. U.S. Geological Survey.

Woodsworth, G. J., Anderson, R. G., & Armstrong, R. L. (1991). Plutonic regimes, chapter 15. In H. Gabrielse, & C. J. Yorath (Eds.), *Geology of the Cordilleran orogen in Canada (Geology of Canada*, Vol. 4, pp. 491–531). Geological Survey of Canada.

Yukon Geological Survey. (2020a). *Yukon digital bedrock geology*. Yukon Geological Survey. Retrieved from http://datatest.geology.gov.yk.ca/Compilation/3

Yukon Geological Survey. (2020b). *Yukon MINFILE – A database of mineral occurrences*. Yukon Geological Survey. Retrieved from http://datatest.geology.gov.yk.ca/Compilation/24

Yukon Geological Survey. (2020c). *Yukon geochronology – A database of Yukon isotopic age determinations*. Yukon Geological Survey. Retrieved from http://data.geology.gov.yk.ca/Compilation/22

Zen, E.-a., & Hammarstrom, J. M. (1984). Magmatic epidote and its petrologic significance. *Geology*, *12*, 515–518. https://doi.org/10.1130/0091-7613(1984)12<515:MEAIPS>2.0.CO;2